land

MDPI

Article

Soybean (*Glycine max*) Cropland Suitability Analysis in Subtropical Desert Climate through GIS-Based Multicriteria Analysis and Sentinel-2 Multispectral Imaging

Noman Ahmad [1,†], Fazila Younas [2,†], Hamaad Raza Ahmad [1,†], Muhammad Sarfraz [3], Muhammad Ashar Ayub [4], Muhammad Aamer Maqsood [1], Fahd Rasul [5], Muhammad Fahad Sardar [6,*], Tariq Mehmood [7], Jamaan S. Ajarem [8], Saleh n. Maoda [8], Xiang Li [9] and Zhaojie Cui [2,*]

1 Institute of Soil and Environmental Sciences, University of Agriculture Faisalabad, Faisalabad 38040, Pakistan; 2017ag9824@uaf.edu.pk (N.A.); hamaadkhan@uaf.edu.pk (H.R.A.); mohamgill@uaf.edu.pk (M.A.M.)
2 School of Environmental Science and Engineering, Shandong University, Qingdao 266237, China; 2015ag441@uaf.edu.pk or fazila.younas@gmail.com
3 Soil Salinity Research Institute, Pindi Bhattian, Hafizabad 52180, Pakistan
4 Institute of Agro-Industry and Environment, The Islamia University of Bahawalpur, Bahawalpur 63100, Pakistan
5 Department of Agronomy, University of Agriculture Faisalabad, Faisalabad 38040, Pakistan
6 Key Laboratory of Ecological Prewarning, Protection and Restoration of Bohai Sea, Ministry of Natural Resources, School of Life Sciences, Shandong University, Qingdao 266237, China
7 Helmholtz Centre for Environmental Research—UFZ, Department of Environmental Engineering, Permoserstr 15, D-04318 Leipzig, Germany; tariq.mehmood@ufz.de
8 Zoology Department, College of Science, King Saud University, Riyadh 11451, Saudi Arabia
9 College of Landscape Architecture and Art, Northwest A&F University, Yangling 712100, China
* Correspondence: fahadsardar16@yahoo.com or fahadsardar@sdu.edu.cn (M.F.S.); cuizj@sdu.edu.cn (Z.C.)
† These authors contributed equally to this work.

check for updates

Citation: Ahmad, N.; Younas, F.; Ahmad, H.R.; Sarfraz, M.; Ayub, M.A.; Maqsood, M.A.; Rasul, F.; Sardar, M.F.; Mehmood, T.; Ajarem, J.S.; et al. Soybean (*Glycine max*) Cropland Suitability Analysis in Subtropical Desert Climate through GIS-Based Multicriteria Analysis and Sentinel-2 Multispectral Imaging. *Land* **2023**, *12*, 2034. https://doi.org/10.3390/land12112034

Academic Editors: Ivan Plaščak, Mladen Jurišić and Dorijan Radočaj

Received: 2 October 2023
Revised: 1 November 2023
Accepted: 2 November 2023
Published: 8 November 2023

Abstract: Soybean (*Glycine max*) is a protein-rich oilseed crop that is extensively used for cooking oil and poultry feed and faces significant challenges due to adverse global climatic conditions aggravated by the ongoing climate crisis. In response to this critical issue, this study was initiated to assess suitable zones for soybean cultivation, aiming to facilitate informed land use decisions within the semi-arid terrestrial ecosystem. Through the utilization of geostatistical interpolation, data layers encompassing soil, irrigation water, land use and land cover, topographic features, and climate information were generated and overlaid based on criterion weightage derived from the Analytic Hierarchy Process. The accuracy of land use and land cover was rigorously evaluated, yielding a 70% overall accuracy and a Kappa (K) value of 0.61, signifying an acceptable level of precision. Validation through the Receiver Operating Characteristic curve for soybean crop suitability demonstrated a highly satisfactory area under the curve of 0.738. The study estimates that out of 172,618.66 hectares, approximately 47.46% of the land is highly suitable (S1) for soybean production, followed by 21.36% moderately suitable (S2), 11.91% marginally suitable (S3), 7.00% currently not suitable (N1), and 12.28% permanently not suitable (N2). Conclusively, the findings suggest that the study area exhibits conducive climatic conditions, optimal soil health, and access to quality irrigation water, all of which have the potential to support soybean crops with improved agronomic practices. This investigation offers valuable insights to both farmers and policymakers concerning irrigation water quality, agricultural productivity, and soil degradation.

Keywords: soybean; land suitability; water quality; climatic conditions; weighted overlay analysis; analytical hierarchy process

1. Introduction

Soybean (*Glycine max*) is a leguminous crop native to East Asia that is extensively grown globally, including in Pakistan, due to its high protein content [1]. It is a crucial source of protein for both humans and animals. It is commonly used in animal feed formulations, especially in the poultry industry, as it provides essential amino acids and high-quality bird protein [2]. Recently, Pakistan has encountered crises related to soybean production and availability, and the frequent shortage of soybean meal, a vital ingredient in poultry feed. The soybean shortage in Pakistan primarily results from increasing demand closely tied to the expanding population. This shortage is exacerbated by inadequate domestic plant protein production and competition for land and water with other crops such as wheat and rice, as farmers prioritize profitability and risk.

The scarcity of soybean meal has resulted in higher prices for poultry feed, making it difficult for farmers to maintain their flocks and causing a decline in overall poultry production [3]. In addition, Pakistan has encountered challenges regarding importing soybean products due to fluctuations in global prices and shifts in government policies. Importantly, strict GMO soybean import restrictions in Pakistan have led to a notable reduction in crushing activity, leading to uncertainty and disruptions in the market. According to the Pakistan Soybean Market Overview 2022 report, Pakistan imported 4.8 billion metric tons of soybeans from various countries, worth USD 2.44 billion, in 2021 [4]. This import volume has added more pressure on the challenging economic situation of Pakistan. Thus, there is a need for additional legislative and scientific initiatives to improve domestic soybean production under the current climatic conditions.

In order to make sustainable land use decisions, it is critical to evaluate the soybean cropland suitability of an area based on irrigation water availability, soil quality, and climatic conditions. A land use plan should be implemented using feasible technologies to conduct a reliable evaluation and interpretation of appropriate, valid, and precise natural resource databases [5]. In the case of land suitability analysis (LSA), choosing the most suitable site for crop production is a complicated process that includes technical criteria and physical, socioeconomic, political, and climatic preferences, which may result in contradictory demands. Such complexities necessitate using multiple decision-support tools simultaneously [6]. Thus, geographic information system (GIS) is a multipurpose tool increasingly employed as a powerful spatiotemporal decision-making system for land suitability assessment, assisting in the proper handling of such detailed and diverse maps [7].

In crop suitability analysis, two powerful techniques, the Analytic Hierarchy Process (AHP) and Weighted Overlay Analysis, stand out. AHP integrates expert knowledge and stakeholder preferences while structuring criteria hierarchically [8]. Weighted Overlay Analysis, a GIS method, efficiently combines spatial data layers to derive suitability indices. Compared to other methods, AHP excels in capturing expert insights and accommodating multiple criteria, and Weighted Overlay Analysis streamlines spatial data handling [9], collectively enhancing decision-making in crop suitability analysis.

This pioneering study investigates the suitability of soybean cultivation in a unique geographic context encompassing non-conventional soybean crops, offering an innovative and significant contribution to agricultural research with a specific focus on Tehsil Jaranwala, Faisalabad District, Pakistan. It distinguishes itself as the first systematic and rigorous assessment of soybean cultivation potential within the semi-arid terrestrial ecosystem of this region. Leveraging a multi-criteria decision analysis approach, the research seamlessly integrates a wide range of critical datasets, including factors such as soil quality, water availability, climatic conditions, topographic features, and land use and land cover data. While previous studies, such as that of Radočaj et al. [10], have utilized a land evaluation model (LEM), this research aligns with the methodology proposed by Kamkar et al. [11] by employing weighted overlay analysis (WOA), providing a streamlined approach involving the assignment of weights to individual criteria and synthesizing these diverse factors into a single suitability score. In essence, this study represents a substantial and rigorous contribution to the field of land suitability assessment, delivering a comprehensive and accurate evaluation of land suitability for soybean cultivation within the unique context of Tehsil Jaranwala, Faisalabad District, Pakistan. This research also fills a critical gap as no similar work has been reported for the agro-ecological regions of Pakistan regarding soybean cultivation, making it a necessary and timely endeavor to identify the most suitable regions for soybean cultivation in the Faisalabad District (Punjab, Pakistan).

2. Materials and Methods

2.1. Site Description

The research site was Jaranwala, located in the Faisalabad District, Pakistan, at 31°20′10.0″ N 73°25′22.0″ E and an altitude of 188 m above sea level, covering an area of approximately 1726.69 km^2 (Figure 1). It is a region of climatic diversity, with its monthly mean temperature varying between chilly and hot and fluctuating annual rainfall, as depicted in Figure S1. This region is renowned for its fertile agricultural land, contributing significantly to Pakistan's economy by producing main crops such as wheat, rice, sugarcane, and vegetables, while the availability of Lower Gogera Branch and Burala Branch irrigation water resources has enabled farmers to cultivate crops all year round.

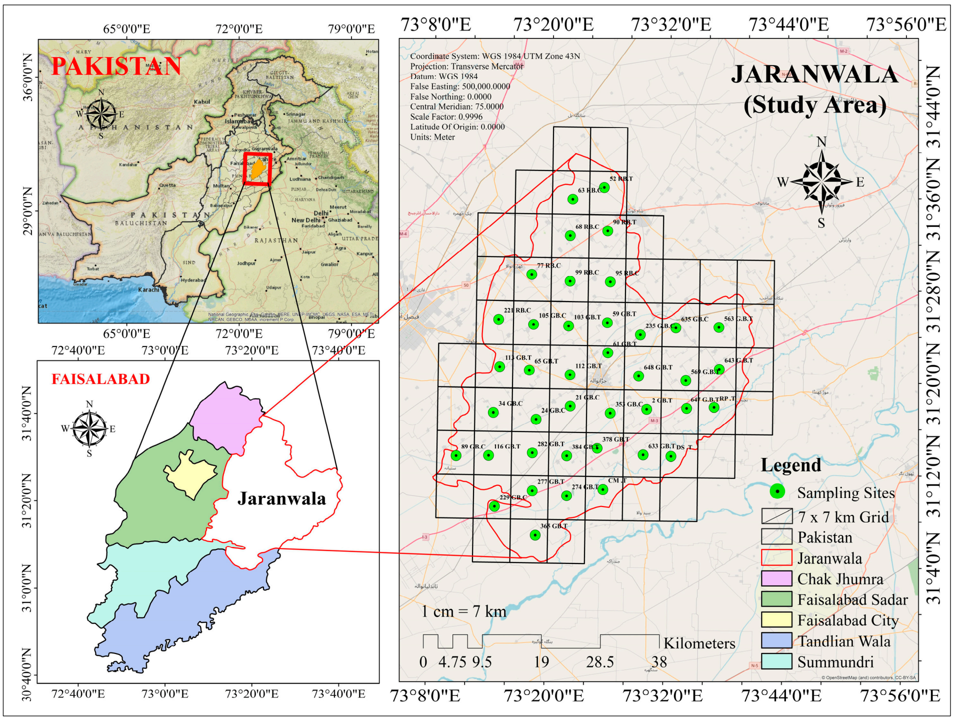

Figure 1. Map of the study area with sampling sites arranged in 7 × 7 grids.

2.2. Methodological Framework

The methodology can be outlined in three primary phases: first, data collection and database creation; second, the application of the Analytical Hierarchy Process (AHP) and Weighted Overlay Analysis (WOA); and finally, the evaluation of cropland suitability, delineated through a series of steps (as depicted in Figure S2).

2.3. Soil and Water Sampling

The boundary of the study area was delineated through digitization using ArcGIS 10.5 software (Esri, Redlands, California, United States), followed by drawing 7 × 7 km grids. A total of 40 sampling sites, with each sample taken from a specific pinpoint location (as shown in Table S1) within a designated grid, were selected to collect soil samples (at a depth of 0 to 15 cm) and available irrigation water (IW) samples, each spaced by 7 km intervals, as illustrated in Figure 1. This sampling strategy was designed to facilitate systematic data collection with precision to ensure accurate results and reduce the potential for sampling errors.

2.4. Irrigation Water Quality Analysis

Irrigation water quality analysis was performed by following the standard methods as described in USDA Agriculture Handbook No. 60. The pH of IW samples was determined using a BANTE PHS-25CW benchtop meter, and the EC (dS m^{-1}) was calculated using a calibrated digital DDS-307W meter (BANTE, Shanghai, China). A hand-held TDS-3 (HM Digital, Carson, California, United States) meter was used to measure the irrigation water TDS (ppm), and the titrimetric method was followed to analyze carbonates ($CO_3{}^{2-}$), bicarbonates ($HCO_3{}^{-}$), chloride (Cl^-), and total hardness (Ca^{2+} + Mg^{2+}) using the methods outlined by Richards [12].

Residual sodium carbonate (RSC) is an indirect property of water, indicating its potential alkalinity or salinity for irrigation purposes. It is calculated in meL^{-1} as follows:

$$\mathrm{RSC}\left(\mathrm{meL}^{-1}\right) = \left(\mathrm{CO}_3^{-2} + \mathrm{HCO}_2^{-1}\right) - \left(\mathrm{Ca}^{2+} + \mathrm{Mg}^{2+}\right) \quad (1)$$

The sodium adsorption ratio (SAR) is a relative proportion of Na^+ ions to Ca^{2+} + Mg^{2+} ions in IW. It predicts how much Na^+ will build up in soil at the expense of Ca^{2+} + Mg^{2+} and K^+ ions due to the regular use of sodic IW. It is stated as follows:

$$SAR\left(\mathrm{mmolL}^{-1}\right)^{1/2} = \frac{\mathrm{Na}^+}{\sqrt{\frac{\mathrm{Ca}^{2+} + \mathrm{Mg}^{2+}}{2}}} \quad (2)$$

2.5. Soil Health Analysis

To measure soil reactions (pH_s), 2 mm sieved air-dried soil-saturated paste was utilized, and the EC_e (dS m^{-1}) of saturated paste extract was determined. The soil extract was analyzed for Na^+ and Ca^{2+} + Mg^{2+} to calculate the soil SAR, following the same procedure described in Section 2.4. The relative proportion of sand, silt, and clay in the soil samples was determined using the hydrometer method [13], and the USDA [14] soil textural classification system was used to evaluate soil texture. A famous gravimetric method was utilized to determine the soil saturation (%) [15]. The soil saturation (%) was calculated using the following formula:

$$SSP(\%) = \frac{Container\ weight\ with\ saturated\ soil\ paste - Container\ weight}{Dry\ soil\ weight - Container\ weight} \times 100 \quad (3)$$

The Walkley and Black [16] wet oxidation method was employed to measure the soil organic matter (%). The plant-available soil phosphorus (mg kg^{-1}) was determined using an APFL (PD-303S), Saitama, Japan spectrophotometer, and a standard curve at a wavelength of 882 nm, as described by Olsen [17]. The extractable K^+ was determined using a flame photometer (Model DV-710), acquired from Digiflame company located in Carpi, Italy, to detect the emission at a specific wavelength of 766.5 nm using the NH_4-acetate method established by Schollenberger and Simon [18].

2.6. Topographic Features and Climate Variables

The Digital Elevation Model (DEM) is a standard tool used in geological sciences to represent terrain elevations in 3D. The Shuttle Radar Topography Mission (STRM) void-filled DEM data for the study area was downloaded from the USGS Earth Explorer (https://earthexplorer.usgs.gov/; accessed on 26 March 2022) website and processed for elevation (m) and slope (%) in ArcGIS 10.5 software, as illustrated in Figure 2a,b. Ten-year mean annual climatological met data with 2 m resolution, allowing highly detailed and accurate representation of climate variables, was collected for temperature and precipitation using the NASA enhanced power Data Access Viewer (DAV) (https://power.larc.nasa.gov/data-access-viewer/; accessed on 13 January 2023) to generate a climate suitability map, as depicted in Figure 2c,d.

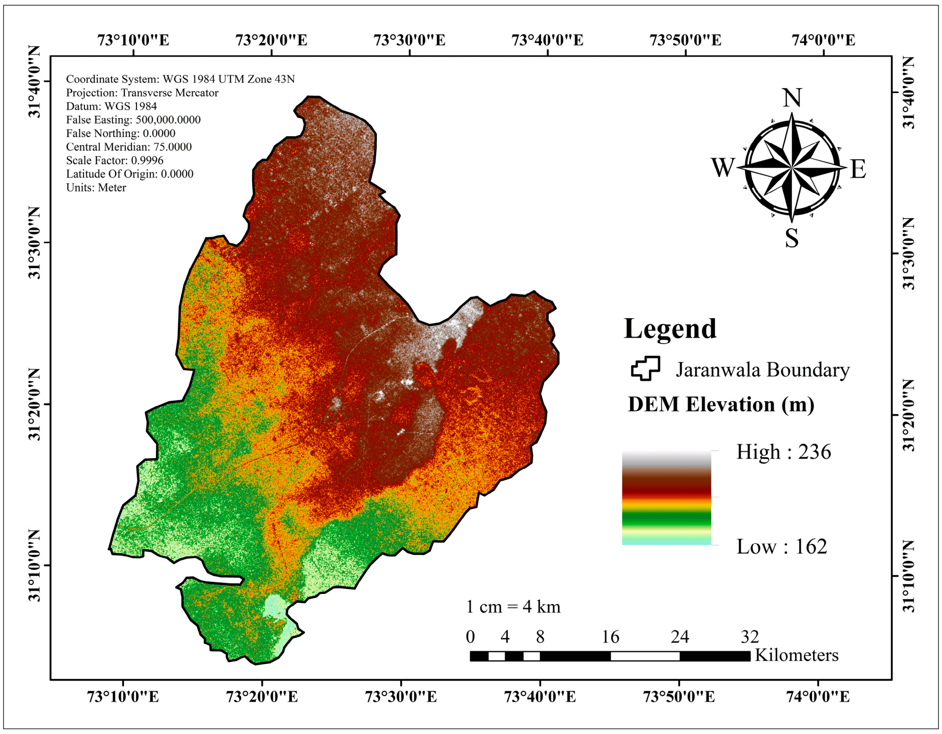

(**a**)

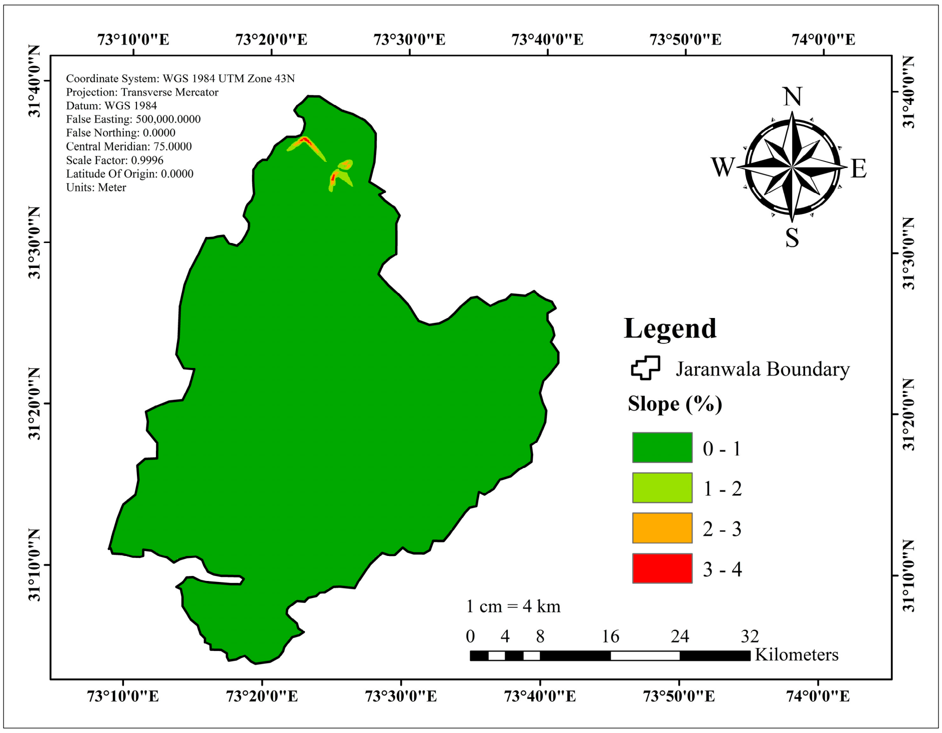

(**b**)

Figure 2. *Cont.*

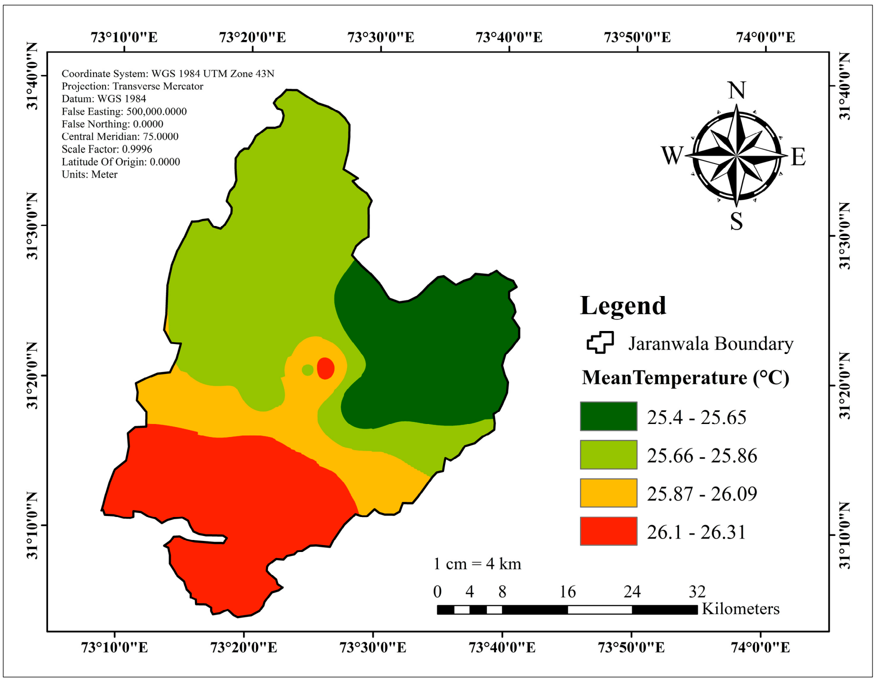

(**c**)

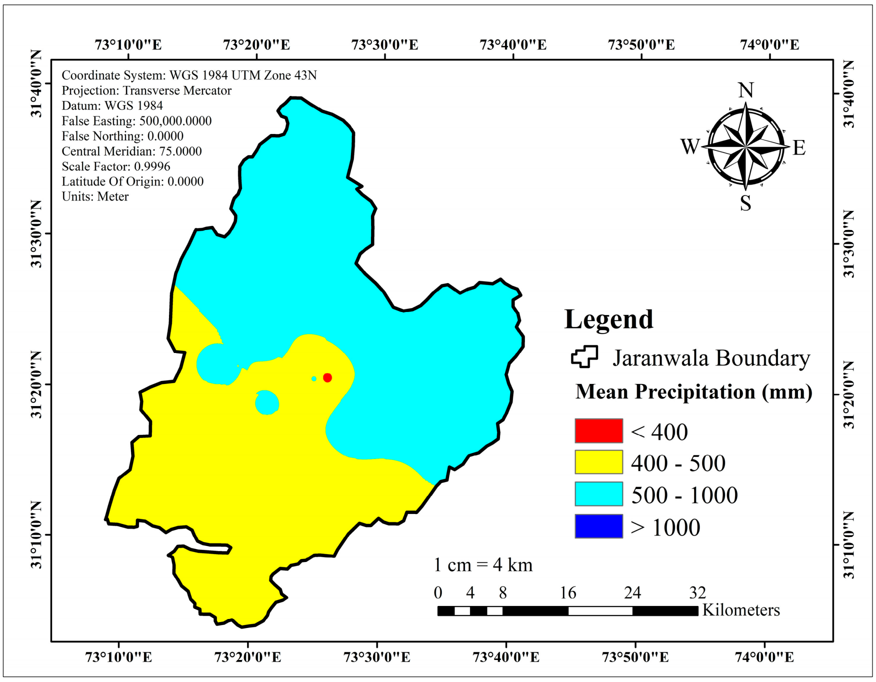

(**d**)

Figure 2. Maps displaying (**a**) elevation and (**b**) slope, along with (**c**) temperature and (**d**) precipitation variables.

2.7. Land Use and Land Cover (LULC)

On 26 March 2022, at 05:46:39 UTC, Sentinel-2A satellite images with a resolution of 10 m (blue, green, red, and near-infrared bands) were acquired from the USGS Earth Explorer portal for the study area, with less than 10% cloud cover. In ArcGIS 10.5, image enhancement was achieved by integrating the image-sharpening panchromatic band-8, available in the Sentinel-2A images package download from the USGS Earth Explorer data portal (https://earthexplorer.usgs.gov/; accessed on 26 March 2022), and using a contrast-stretching technique to enhance the visual quality of satellite images, as recommended by [19,20]. This study used supervised classification with support from ground truth data during field surveys and incorporated high-resolution Google Earth images to classify the different Land Use and Land Cover (LU/LC) classes existing in the study area (Figure 3). To accomplish this, representative sampling sites of known cover types, called training areas, were used to create parametric signatures of each class. The Maximum Likelihood Classification algorithm, a widely recognized approach in remote sensing, was then used to numerically compare each pixel in the dataset to each category in the interpretation key and assign the name of the category to which it was most similar [21].

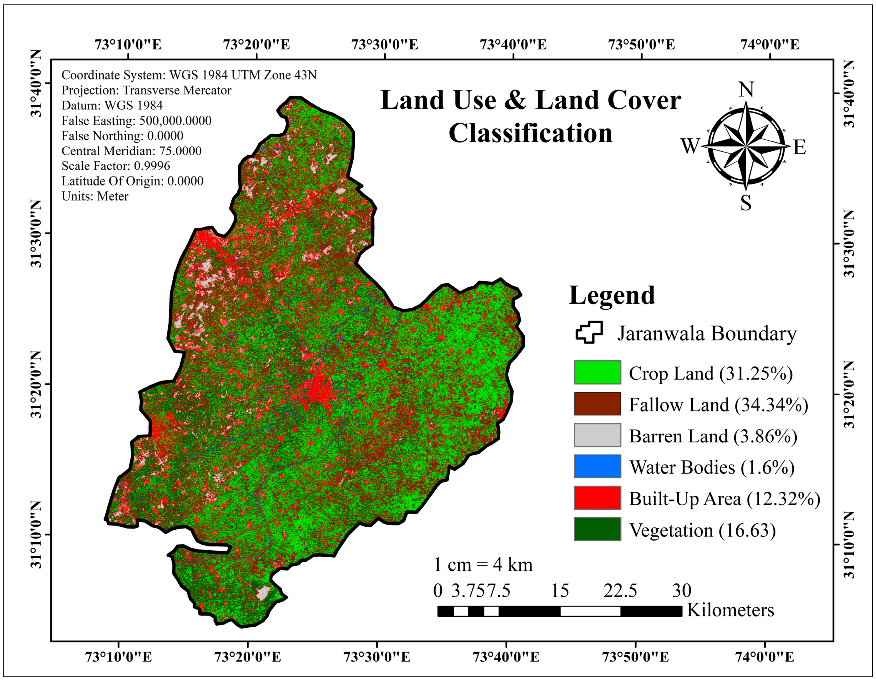

Figure 3. Spatial distribution of land use and cover types in the study area.

2.8. LU/LC Classification Accuracy Assessment

The crucial final step in the classification process involves accuracy assessment. Figure S3 illustrates the schematic of the workflow for LU/LC classification and accuracy assessment. Its primary objective is to quantitatively evaluate the effectiveness of pixel sampling for correct LC&LU classification. We established 40 random points within the study area's classified image. Real-time ground truth data was used to fill the accuracy assessment reference column, serving as the definitive reference for point classification. Figure S4 illustrates the connection between ground truth data and the corresponding classified data derived from the confusion/error matrix report.

Table S2 presents a theoretical error matrix for a LU/LC classification. It shows how pixels in the validation set are assigned to classes (ground truth) and compares this to their assignment in the image. The diagonal represents correct classifications, while off-diagonal elements in the rows indicate commission errors, signifying confusion between the classes. Additional metrics in Table S3 provide further accuracy details. The study also computes various statistics, including the overall Kappa statistic from [22], which measures agreement. A Kappa coefficient of one implies perfect agreement, while a value near zero suggests chance-level agreement (Table S4). Refer to [23–25] for more in-depth information.

2.9. Geostatistical Analysis

In the present study, Inverse Distance Weighted (IDW) interpolation was used to predict the spatial distribution of soil and water characteristics (except texture), topographic features, and climatic data using ArcGIS 10.5 software. The USDA texture scheme and Soil

Texture Plugin of QGIS 2.18.22 software were used to create a soil texture map from input sand, silt, and clay raster files, as illustrated in Figure 4.

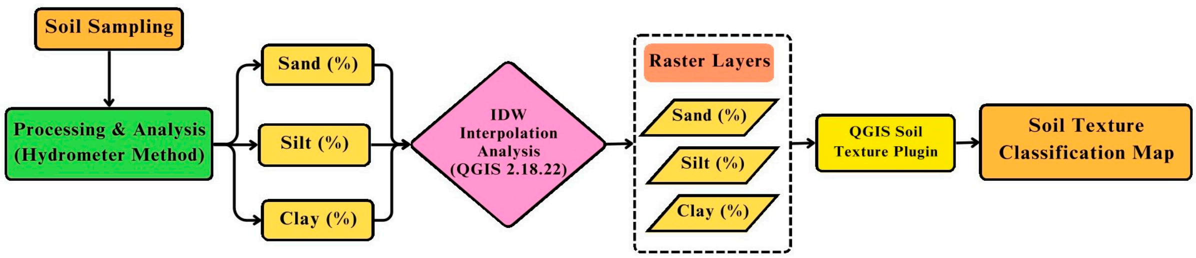

Figure 4. A workflow diagram for mapping and classifying soil textures.

2.10. Decision-Making Process

In the decision-making process, Table S8 serves as a comprehensive resource presenting an overview of datasets and thematic maps, complete with sources, resolutions, and pertinent information. Detailed information on the hierarchical organization of criteria, standardization of criteria, and the Multicriteria Weighted Overlay Analysis (MCWOA) is provided below.

2.10.1. Hierarchical Organization of Criteria

Analytic Hierarchy Process (AHP) is a decision-making technique that involves breaking down complex problems into a hierarchical structure of criteria, sub-criteria, and alternatives [26]. This study demonstrates the spatial AHP procedure using a typical four-level hierarchy of goals, objectives, attributes, and alternatives (Figure S5). A matrix for pairwise comparison was created to evaluate the main criteria, with input obtained from experts, public institutions, and stakeholders. The opinions received were scored using binary comparisons, and the criteria were weighed on a scale of 1–9, as shown in Table 1. This scoring system is based on previous studies [8,27]. The pairwise comparison matrix was assessed using the Consistency Ratio (CR) index to ensure consistency. The CR index measures the matrix's degree while accommodating both consistent and inconsistent interactions. The studies conducted by Chen [28] have shown that the value of CR depends on the Consistency Index (CI) and Ratio Index (RI), as given below:

$$Consistency\ Ratio\ (CR) = \frac{Consistency\ Index\ (CI)}{Ratio\ Index\ (RI)} \tag{4}$$

$$Ratio\ Index\ (RI) = \frac{\lambda_{max} - n}{n-1} \tag{5}$$

where λ_{max} indicates the maximal eigenvector and n denotes the rank of the matrix. As discussed by Prasad and Kousalya [29], if the pairwise comparison matrix obtained does not satisfy Saaty's CR condition (<10%), decision-makers must revise their decisions. Saaty [8] demonstrates that the weight values in Figure 5a–c, calculated by using the AHP technique as given in Tables S4, S5, and S7, are logically reasonable based on CR (%).

Table 1. The SAATY 1–9 scale for pairwise comparisons study.

Magnitude	Numeric Score	Reciprocal
Equally important	1	1
Moderately important	3	1/3
Strongly important	5	1/5
Demonstrated importance	7	1/7
Absolutely important	9	1/9
Intermediate or transition values	2, 4, 6, and 8	1/2, 1/4, 1/6, and 1/8

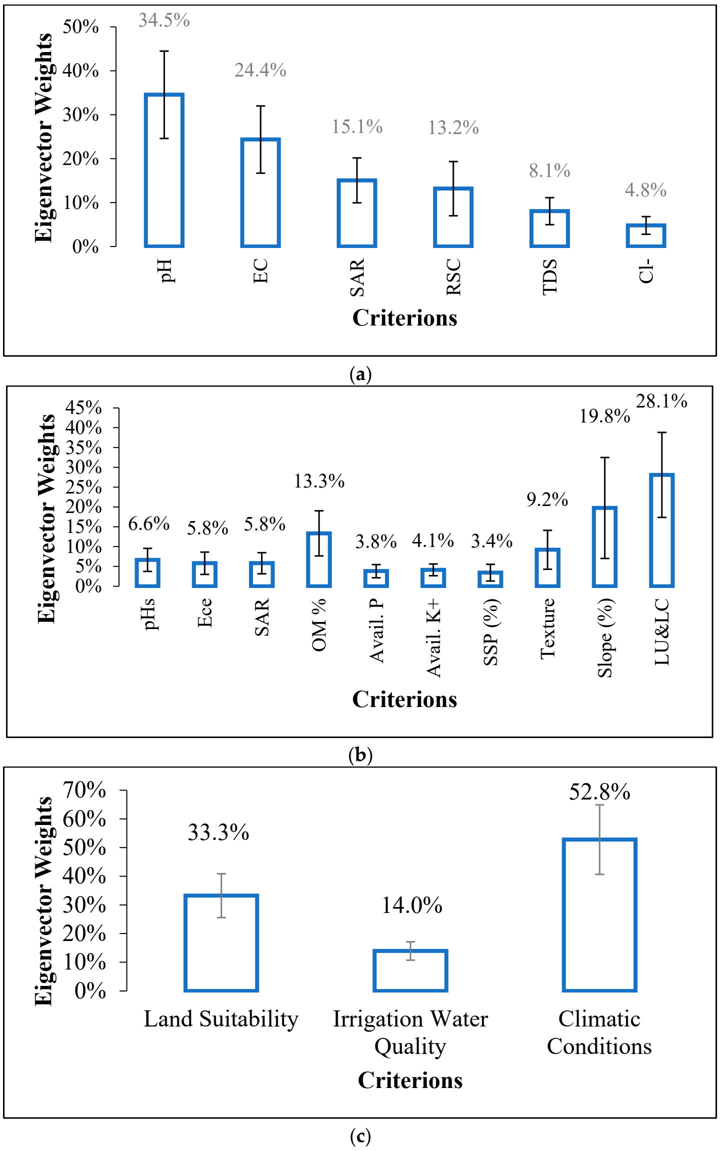

Figure 5. Assigned weightage values to each factor for (**a**) irrigation water suitability; (**b**) land suitable for soybean cultivation, and (**c**) soybean crop suitability.

2.10.2. Standardization of Criteria

During the standardization process, mapping units were classified using the FAO guidelines for land-use planning, as shown in Table S9. For the assessment of soil health, IW quality, climate, and topographic features suitability, mapping units were classified using expert opinion, FAO criteria, and the Soil Fertility Research Institute of Pakistan (SFRI) manual, and to classify mapping units for the evaluation of land suitability for soybean crops, various academic studies were consulted in addition to expert opinions, as shown in Table S10.

2.10.3. Multicriteria Weighted Overlay Analysis (MCWOA)

MCWOA is a GIS-based technique used to assess the suitability of different zones for a specific land use or management option [30]. This method combines multiple input layers to generate an output map, with each location ranked based on its overall suitability for the decision at hand [31]. The relevant decision criteria were identified in this study, and separate thematic layers were created. Each layer was standardized by rescaling the values to a common scale ranging from 1 to 5. All layers were combined in ArcGIS 10.5 software using the weighted overlay tool to generate a composite suitability map that reflects the relative importance of each criterion.

2.10.4. Model Accuracy Assessment

When employing the AHP framework for classification tasks, such as object grouping based on computed weights, the area under the receiver operating characteristic (ROC–AUC) curve is commonly used to validate conclusions [32]. In AHP-based cropland suitability analysis, ROC–AUC assesses the AHP model's performance in categorizing suitable zones based on provided weights and variables [33]. It involves ROC curve calculation by adjusting classification thresholds for potential zones and determining the AUC to differentiate high and low potential zones [34].

Validation in the Analytic Hierarchy Process (AHP) involves gathering testing samples (True Positive Rate) from field surveys or secondary data sources to establish training sets for the AUC-ROC curve evaluation, as depicted in Figure S6. Suitability analysis was performed using AHP and Weighted Overlay to create a suitability raster map (False Positive Rate), later categorized into 'Suitable' and 'Not Suitable'. Both the testing samples and the binary suitability raster were reprojected to a shared UTM Zone 43N coordinate system for easy comparison. Finally, the ArcSDM tool was utilized to compute the AUC-ROC curve, assessing the relationship between the True Positive Rate and False Positive Rate (Figure S7).

3. Results

3.1. Water Quality Evaluation

This evaluation entails gathering, analyzing, and visualizing data on factors that can influence the quality of irrigation water (IW) by using GIS and RS techniques. Table 2 shows the pH values of IW samples, which ranged from 6.30 to 8.90, and spatial distribution results revealed that 83.97% of the total 172,618.66 ha falls in the S1 FAO classification category and 0.07% in the N2 category (Figure 6a). Groundwater quality is typically assessed using electrical conductivity (EC), which is a major concern in the Indian subcontinent. The results showed that the EC of IW samples ranged from non-saline (0.18 dS m^{-1}) to very slightly saline (2.48 dS m^{-1}), as shown in Figure 6b, with most of the study area falling into the S2 (47.32%) and S3 (50.31%) categories (Table 2).

Table 2. Irrigation water hierarchical structure with suitability classes, scores, and covered areas.

		Irrigation Water Suitability				
Main Criteria	**Unit**	**Sub-Criteria**	**Suitability Class**	**Score**	**Hectare Coverage**	**Area (%)**
pH	-	6.0–6.5	S1	1	144,946.31	83.97
		6.5–7.5	S2	1	25,195.17	14.60
		7.5–8.0	S3	2	2049.49	1.19
		8.0–8.5	N1	3	427.68	0.18
		>8.5	N2	4	120.83	0.07
EC	(dS m^{-1})	≤0.25	S1	1	952.76	0.55
		0.25–0.75	S2	2	81,683.15	47.32
		0.75–2.00	S3	3	86,836.52	50.31
		2.00–3.00	N1	4	3146.22	1.82
RSC	(me L^{-1})	≤1.0	S1	1	167,905.67	97.27
		1.0–1.25	S2	2	1329.63	0.77
		1.25–2.0	S3	3	2405.19	1.39
		2.0–2.5	N1	4	978.17	0.57
SAR	(mmol L^{-1})$^{1/2}$	≤10	S1	1	172,030.06	99.66
		10–18	S2	2	588.59	0.34
Chloride	(me L^{-1})	≤4.0	S1	1	136,854.22	79.28
		4.0–7.0	S2	2	27,676.57	16.03
		7.0–12.0	S3	3	8087.86	4.69
TDS	(ppm)	≤200	S1	1	4242.95	2.46
		200–500	S2	2	84,532.96	48.97
		500–1500	S3	3	83,453.17	48.35
		1500–3000	N1	4	389.57	0.23

Water RSC indicates the potential alkalinity or salinity of IW. The findings regarding the RSC of IW, shown in Figure 6c, revealed that the highest RSC value (2.5 me L^{-1}) of N1 quality was observed in tube-well water taken from the boundary of Chak No. 282 GB and 52 RB. However, the remaining area had access to IW with RSC values below the SFRI-specified permissible limit of 1.5 me L^{-1}. SAR measures the abundance of Na^+ in water relative to the soluble divalent ions (Ca^{2+} + Mg^{2+}). The lab analysis revealed that the SAR in the study area IW ranged from 0.00 to 11.19 (Figure 6d), and the spatial analysis indicated that 99.66% of the area has access to S1 quality of IW and 0.34% has access to N1 quality of IW (Table 2).

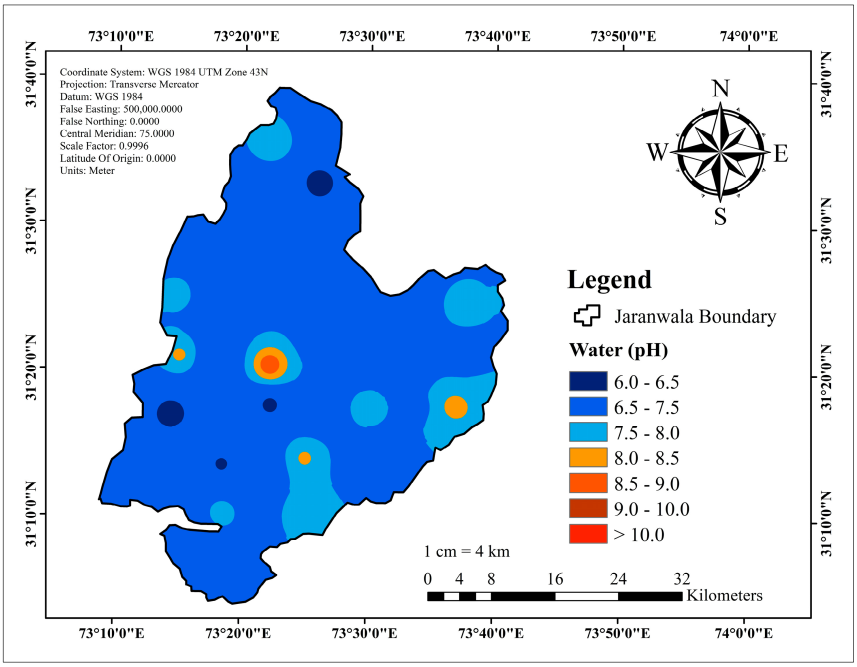

(**a**)

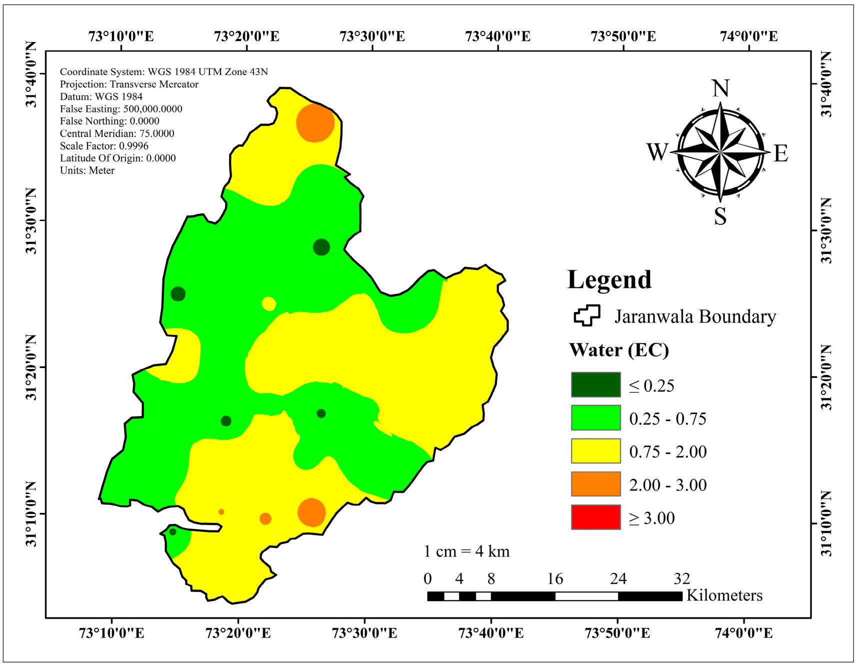

(**b**)

Figure 6. *Cont.*

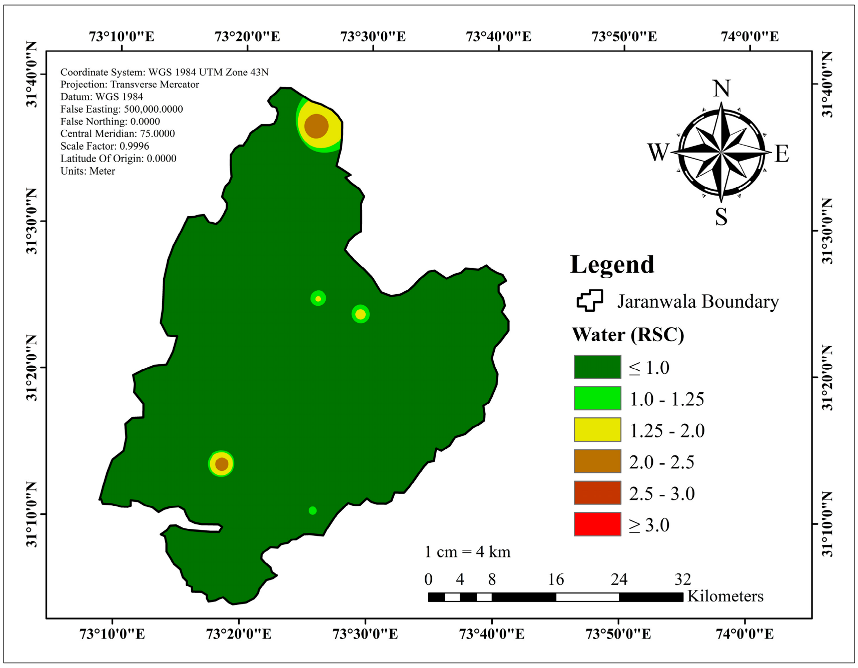

(**c**)

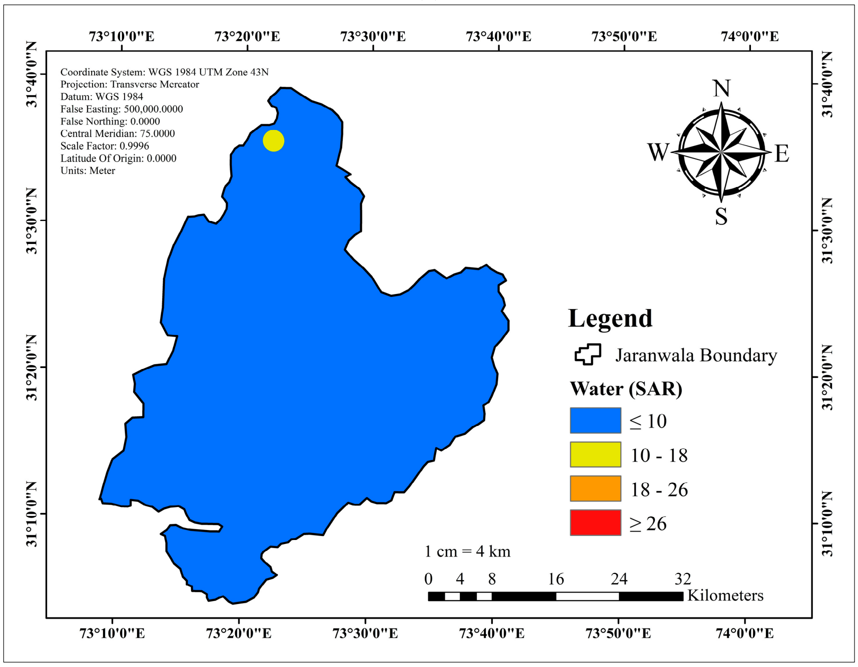

(**d**)

Figure 6. *Cont.*

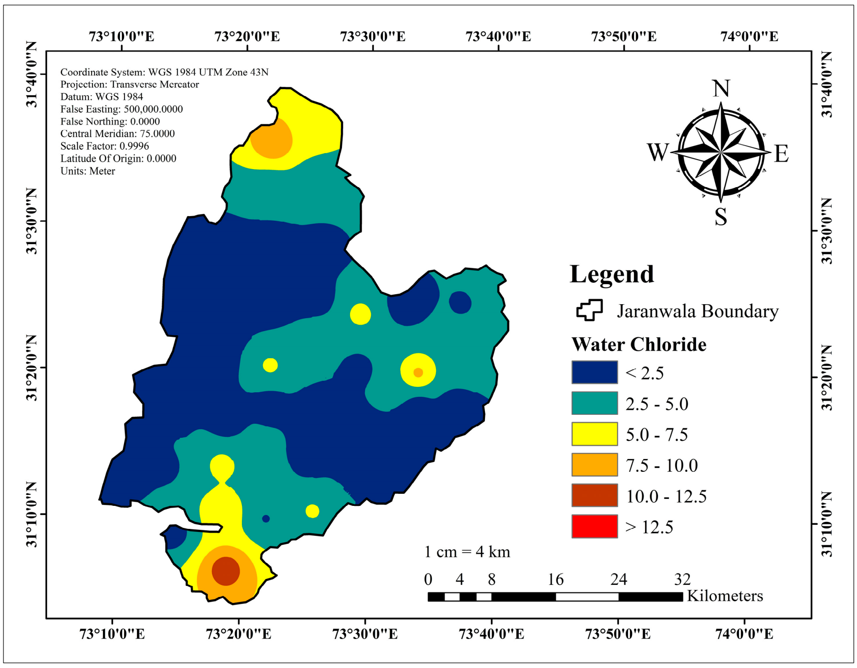

(**e**)

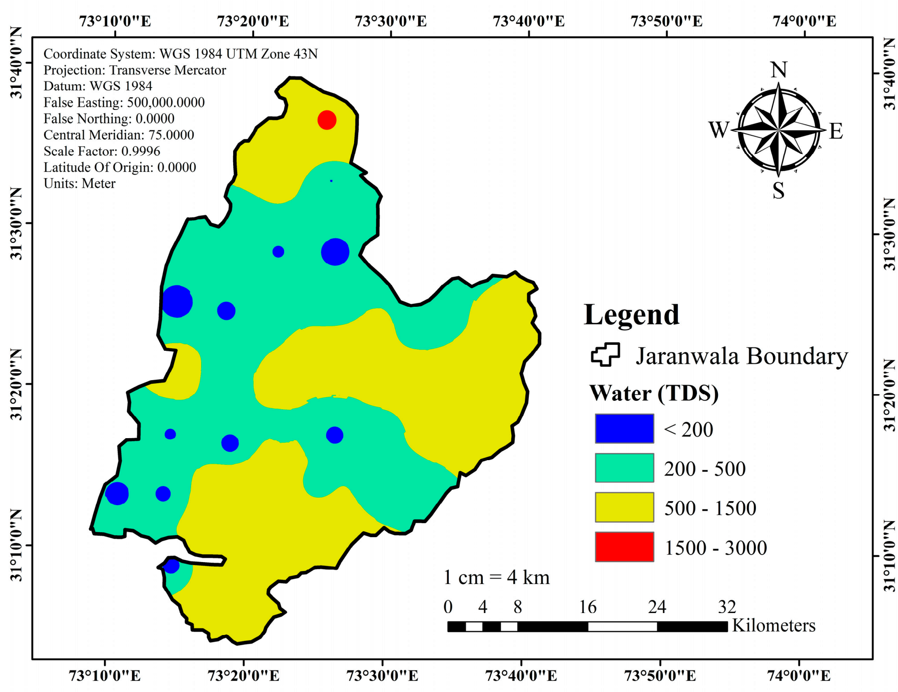

(**f**)

Figure 6. GIS-based standardized irrigation water criterion maps (**a**) water pH; (**b**) electrical conductivity (EC); (**c**) residual sodium carbonate (RSC); (**d**) sodium adsorption ratio (SAR); (**e**) chloride (Cl^-); and (**f**) total dissolved solids (TDS).

3.2. Land Suitability Analysis

Evaluating agricultural land suitability is critical in crop growth and development management. The lab analysis results indicated that the soil pH is primarily alkaline, with pH values ranging from 7.5 to 8.90, as depicted in Figure 7a. The geostatistical analysis indicated that 64.41% of the study area falls in the N1 class, followed by 31.56% in the S3 class of the FAO system (Table 3). The EC_e of the soil-saturated paste extract ranged from 0.03 dS m^{-1} to 4.95 dS m^{-1}, as shown in Figure 7b. The soil quality in terms of EC_e ranged from S1 (76.65%) to S3 (1.30%), as given in Table 3, indicating that soil EC_e is within the acceptable range. SAR in soil samples varied from 0.59 to 36.88, as illustrated in Figure 7c. The IDW analysis estimated that 48.23% of the land in the study area falls into the S1 class and only 0.84% in the N2 class, as given in Table 3.

Plant-available phosphorus and K^+ are essential plant macronutrients. Their concentration is used to determine the soil fertility status. Lab analysis showed that phosphorus content in soils ranged from 2.1 mg kg^{-1} to 24.1 mg kg^{-1}, as illustrated in Figure 7d. According to SFRI criteria, approximately 55.65% of the study area falls in S2, 49.71% in S3, and 3.64% in N1 class (Table 3). On the other hand, NH_4-acetate extracted K^+ varied widely from as low as 60 mg kg^{-1} to as high as 580 mg kg^{-1}, as shown in Figure 7e. Geostatistical interpolation showed that above half of the study area falls under the class of S3 followed by S2, covering an area of 50.79% and 39.94%, respectively (Table 3). Notably, soil OM (%) ranges from 0.4% to 1.37%, as depicted in Figure 7f. Based on the IDW analysis, OM (%) in soils covering 1.15% to 17.70% area ranged from poor to adequate, and most contained no more than 1% (Table 3).

Long-term productivity and profitability in agriculture require adequate soil saturation (%). The analysis results, shown in Table 3, show that the SSP (%) of the study area ranges from 32% to 38% and falls into the S1 and S3 categories, covering 71.20% and 28.80% area, respectively, as shown in Figure 7g. Crop growth depends on soil texture for water retention, nutrient availability, and root development. The soil texture evaluation revealed that loam and clay loam are the most common soil textural classes in the study area as shown in Figure 7k. The textural suitability classification along with the covered area is given in Table 3.

The slope is the inclination or steepness of the ground and is usually measured in percentages. It is essential in pedogenesis and soil conservation because it influences runoff, soil drainage, erosion, machine operations, and crop selection. The DEM data analysis revealed that 99.57% of the study area has slopes less than 1%, and only 0.05% has slopes between 3% and 4% (Table 3). This indicates that approximately 99.57% of the land is classified as S1 in terms of productivity and erosion control (Figure 2b). The LU/LC type in the study area includes cropland, fallow land, barren land, water bodies, built-up areas, and forest/vegetation, as shown in Figure 3. According to the analysis, approximately 65.59% of the study area is classified as S1, which includes cropland (31.25%) and fallow land (34.34%). Water bodies (1.60%) and built-up areas (12.32%), on the other hand, are classified as N1 and N2 (Table 3).

The land-use and land-cover classification accuracy assessment results in Table S3 reveal valuable insights into the classification model's accuracy and performance. Cropland displayed a low omission error, with only 33.33% of pixels mistakenly excluded, indicating a high user accuracy of 0.91, showcasing the model's proficiency in identifying cropland. in contrast, water bodies and built-up areas showed high commission errors, implying significant misclassification. Producer accuracy was notably high for water bodies and built-up areas, reflecting accurate classification. The Kappa coefficient (K) indicated a substantial overall agreement at 0.61, signifying that the model's performance is quite robust and practical for real-world use, while the 70% overall accuracy (OA) demonstrated the model's effectiveness across all classes. These findings highlight the model's strengths and weaknesses, emphasizing the need to reduce commission errors in water bodies and built-up areas and fine-tune the model for enhanced accuracy and reliability in future applications.

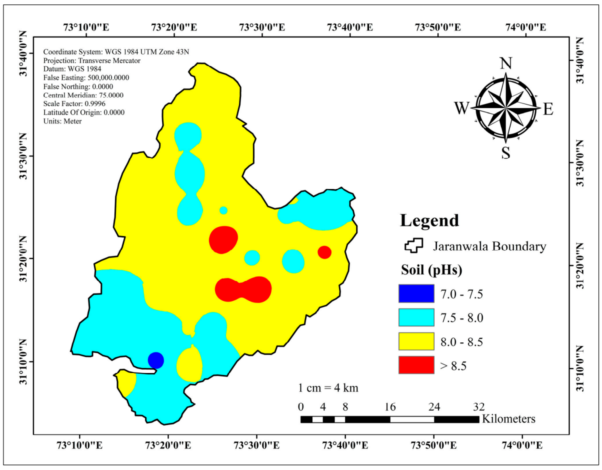

(**a**)

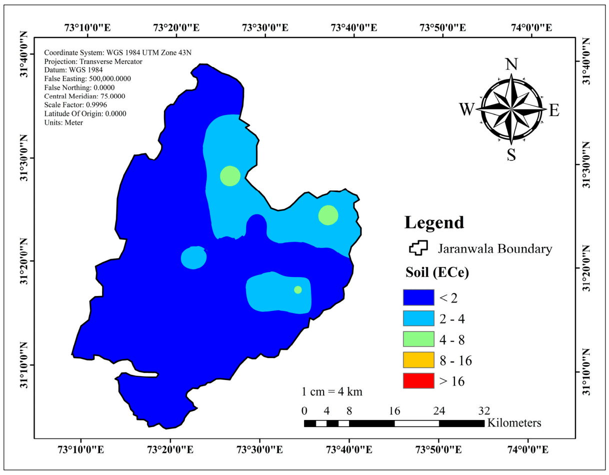

(**b**)

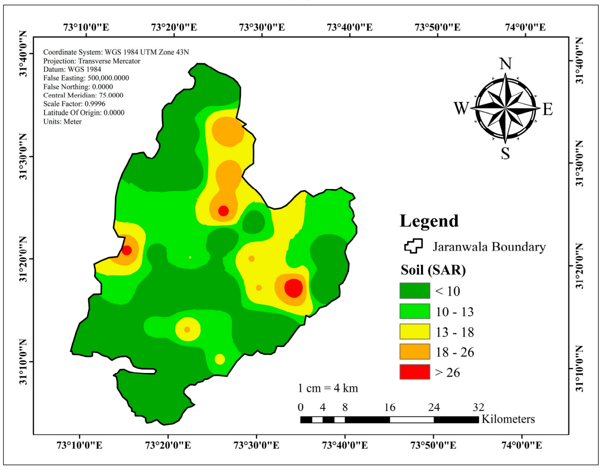

(**c**)

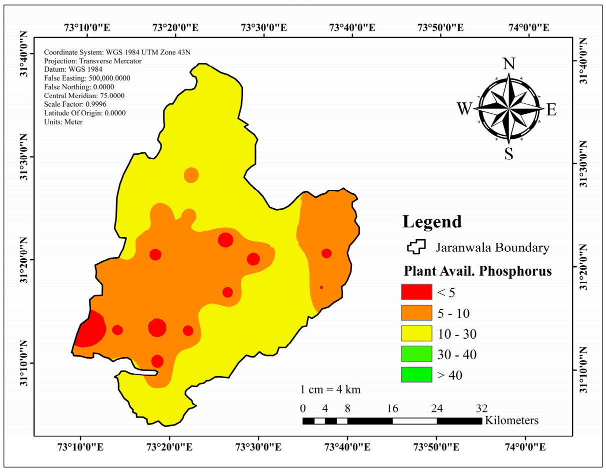

(**d**)

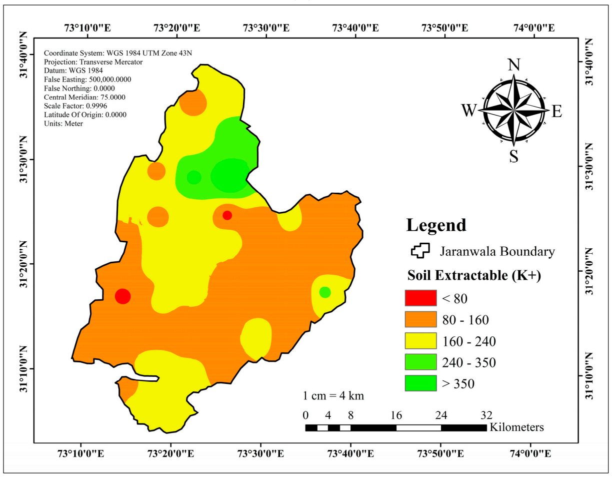

(**e**)

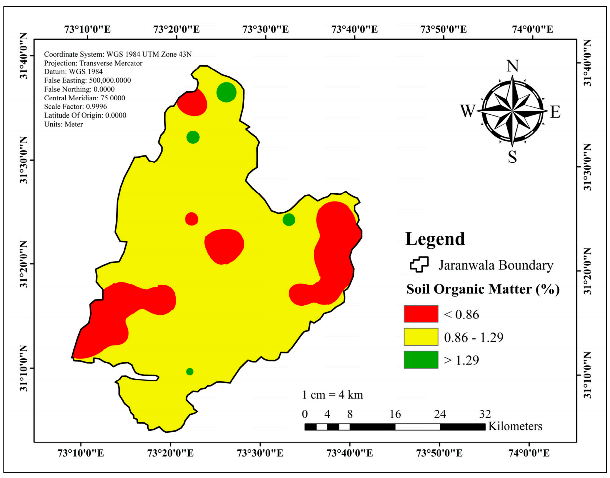

(**f**)

Figure 7. *Cont.*

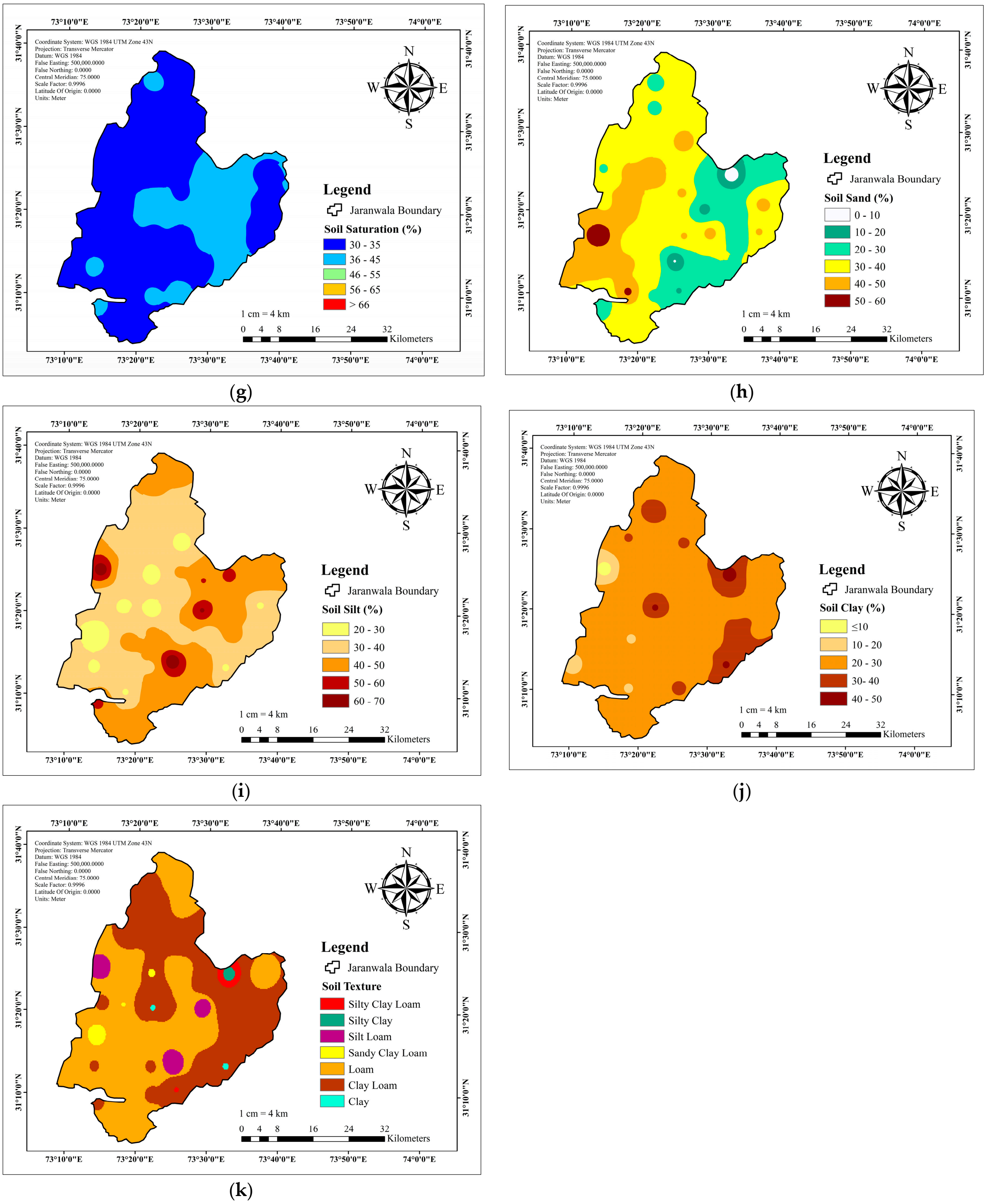

Figure 7. GIS-based standardized criterion maps (**a**) soil pH; (**b**) soil EC_e; (**c**) sodium adsorption ratio (SAR); (**d**) plant-available phosphorus; (**e**) extractable K^+; (**f**) organic matter; (**g**) soil saturation (%); (**h**) soil sand; (**i**) soil silt; (**j**) soil clay; and (**k**) soil texture.

The weightage calculated from AHP analysis for all ten factors, including LU/LC, was used to evaluate agriculture land suitability in the study area. Figure 8a,b shows that more than half of the study area, covering 112,509.76 ha (65.59%), is highly suitable, 28,526.10 ha (16.63%) is moderately suitable, 6562.02 ha (3.83%) is marginally suitable, 2752.92 ha (1.60%) is currently not suitable, and 21,183.19 ha (12.35%) is permanently not suitable for supporting farming practices.

Table 3. Agriculture land and climate hierarchical structure with suitability classes, scores, and covered areas.

Main Criteria	Unit	Sub-Criteria	Suitability Class	Score	Hectare Coverage	Area (%)
Agriculture Land Suitability						
pH_s	-	7.0–7.5	S2	1	669.05	0.39
		7.5–8.0	S3	2	54,485.08	31.56
		8.0–8.5	N1	3	111,184.79	64.41
		>8.5	N2	4	6279.74	3.64
EC_e	($dS\ m^{-1}$)	<2.0	S1	1	132,319.09	76.65
		2.0–4.0	S2	2	38,063.76	22.05
		4.0–8.0	S3	3	2235.81	1.30
SAR	$(mmol\ L^{-1})^{1/2}$	<10.0	S1	1	83,254.10	48.23
		10.0–13.0	S2	2	49,141.20	28.47
		13.0–18.0	S3	3	28,506.50	16.51
		18.0–26.0	N1	4	10,272.90	5.95
		>26.0	N2	5	1443.96	0.84
Soil Saturation	(%)	30.0–35.0	S1	1	122,901.60	71.20
		35.0–45.0	S3	2	49,717.05	28.80
Soil Texture	-	Silt Loam	S1	1	5222.43	3.02
		Sandy Clay Loam	S2	2	1804.59	1.05
		Silty Clay	S2	2	639.72	0.37
		Loam	S1	1	88,478.55	51.24
		Silty Clay Loam	S2	2	1618.56	0.94
		Clay Loam	S2	2	74,629.80	43.22
		Clay	S3	3	272.88	0.16
Slope	(%)	0–1	S1	1	171,960.00	99.57
		1–2	S1	1	464.67	0.27
		2–3	S2	2	184.02	0.11
		3–4	S2	2	88.68	0.05
Plant Avail. Phosphorus	($mg\ kg^{-1}$)	<5.0	N1	4	6275.50	3.64
		5.0–10.0	S3	3	70,279.69	40.71
		10.0–30.0	S2	2	96,063.45	55.65
Extractable (K^+)	($mg\ kg^{-1}$)	<80	N1	4	834.19	0.48
		80–160	S3	3	87,679.20	50.79
		160–240	S2	2	68,937.40	39.94
		240–350	S1	1	11,403.50	6.61
		>350	S1	1	3764.45	2.18
Soil Organic Matter	(%)	<0.86	S3	3	30,560.30	17.70
		0.86–1.29	S2	2	140,072.00	81.15
		>1.29	S1	1	1985.97	1.15
LU/LC Type	-	Crop Land	S1	1	53,967.63	31.25
		Fallow Land	S1	1	59,301.04	34.34
		Forest/Vegetation	S2	2	28,723.20	16.63
		Barren Land	S3	3	6661.44	3.86
		Water Bodies	N1	4	2768.45	1.60
		Built-Up Area	N2	5	21,279.75	12.32
Climate Suitability						
Temperature	(°C)	24–28	S1	1	172,616.43	100
Precipitation	(mm)	<400	S3	3	99.24	0.06
		400–500	S2	2	77,592.61	44.95
		500–1000	S1	1	94,924.58	54.99

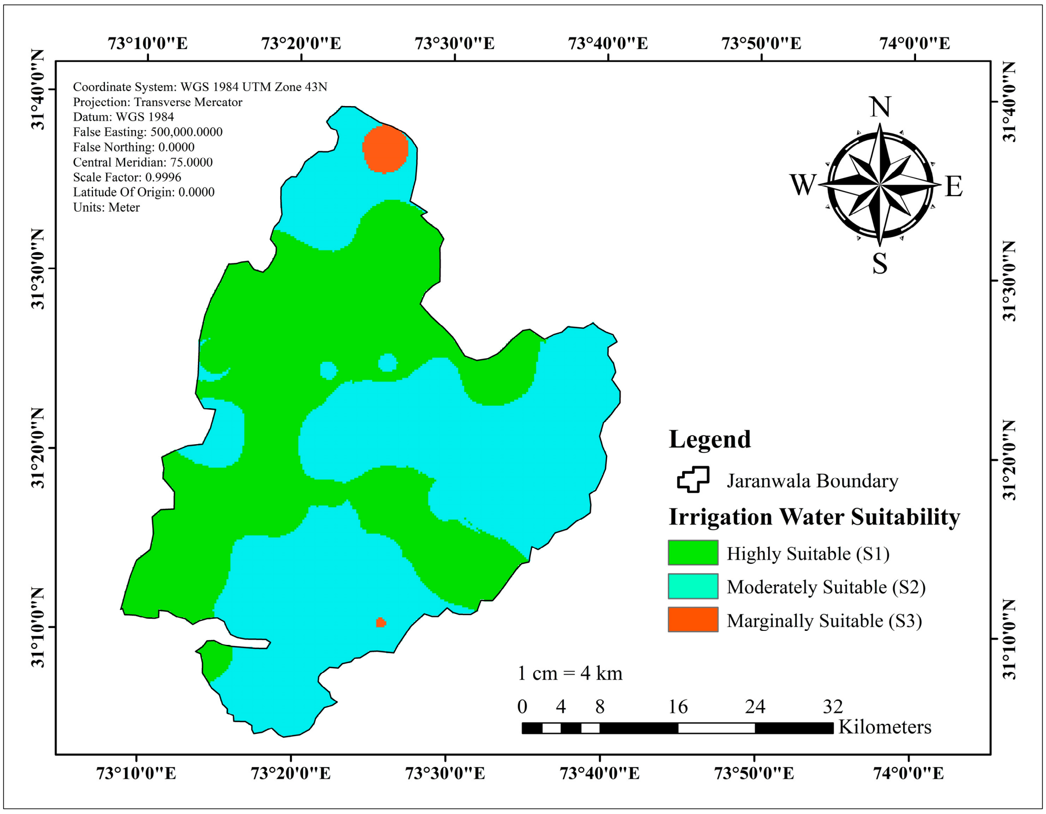

(**a**)

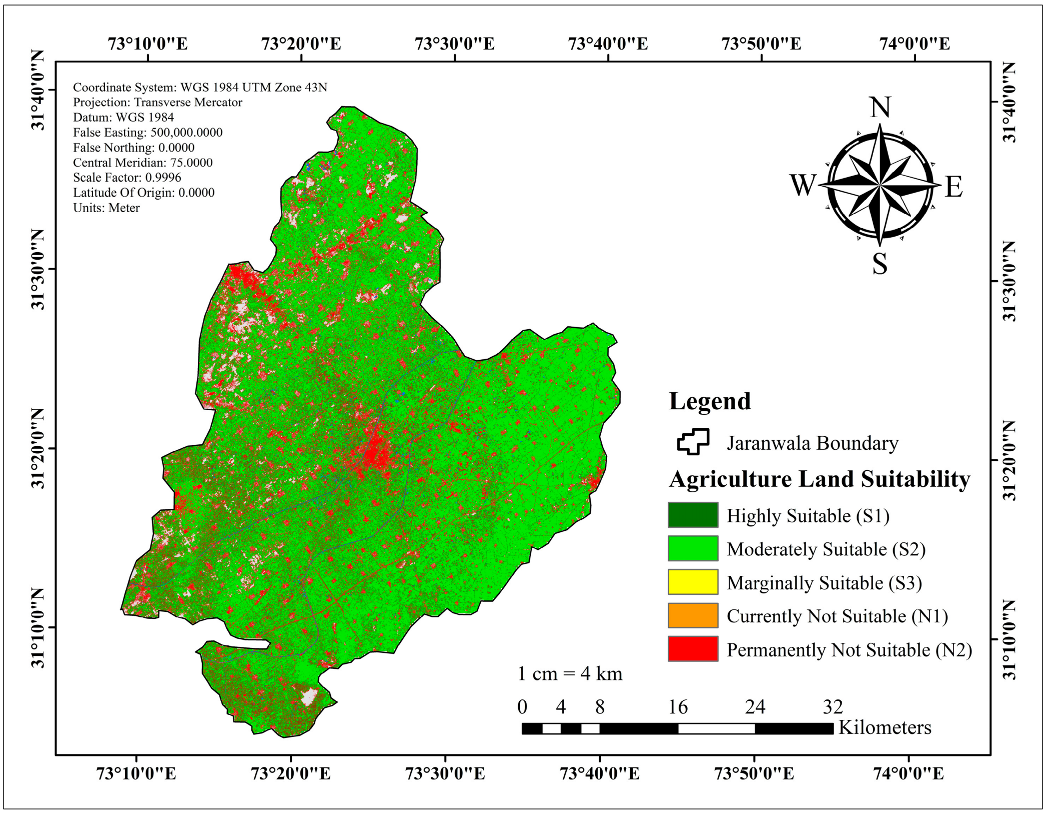

(**b**)

Figure 8. *Cont.*

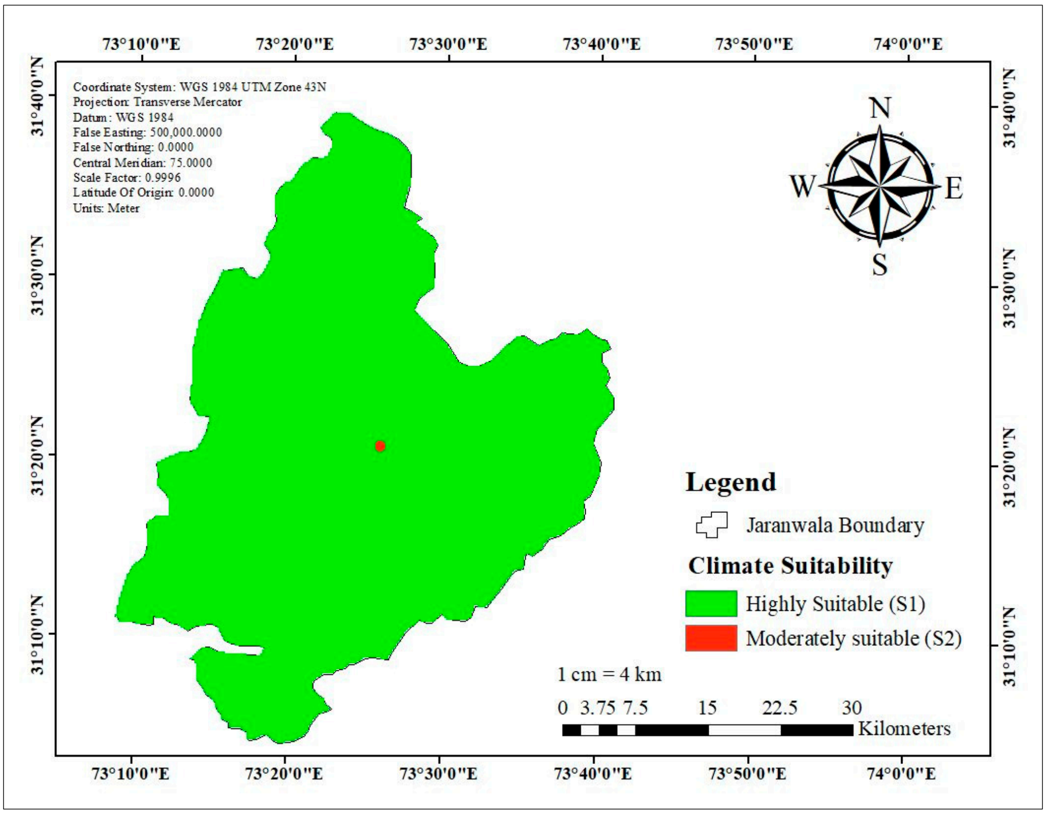

(**c**)

Figure 8. Suitability maps with coverage areas for (**a**) irrigation water; (**b**) agricultural land; and (**c**) climatic conditions.

3.3. Climate Suitability Assessment

The analysis of ten years of climatological data for temperature and precipitation (rain, snowfall, and hailstorm) suitability showed that the mean ten-year temperature varied from as low as 25.40 °C to as high as 26.31 °C, and the precipitation varied from as low as 381.27 mm to as high as 597.75 mm in the region (Tables S11 and S12). The geostatistical interpolation analysis results are shown in Figure 8c.

3.4. Soybean Suitability Analysis

All factors have a different impact on crops. Some crops require a higher concentration of one factor than others. When determining land suitability for soybean production, the factors listed in Table 4 were considered. According to the analysis results, the most promising areas for expanding soybean production within the study area were identified as highly suitable (S1) and moderately suitable (S2), covering an area of 81,524.33 ha (47.46%) and 20,452.01 ha (11.91%), respectively, as shown in Figure 9a,b. Soybean crop suitability (SCS) results validation was conducted using the AUC–ROC (area under the receiver–operating characteristic curve), a widely recognized statistical method. The results of this validation analysis demonstrated a commendable level of reliability, yielding an AUC–ROC value of 0.738, as graphically represented in Figure S7. This suggests that the model can reliably classify and make accurate predictions, laying a strong foundation for its potential application in real-world scenarios.

Table 4. Hierarchical structure for soybean cropland suitability mapping.

Main Criteria	Suitability Class	Score	Hectare Coverage	Area (%)
Irrigation Water	S1	1	79,426.18	46.01
	S2	2	91,028.66	52.73
	S3	3	2163.82	1.25
Agriculture Land	S1	1	112,509.76	65.59
	S2	2	28,526.10	16.63
	S3	3	6562.02	3.83
	N1	4	2752.92	1.60
	N2	5	21,183.19	12.35
Climatic Conditions	S1	1	172,517.00	99.94
	S2	2	99.00	0.06

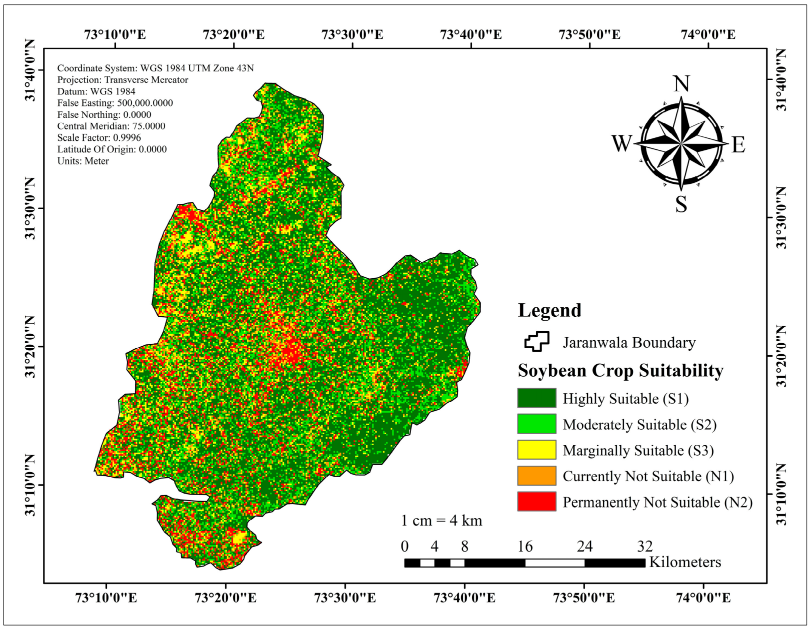

(**a**)

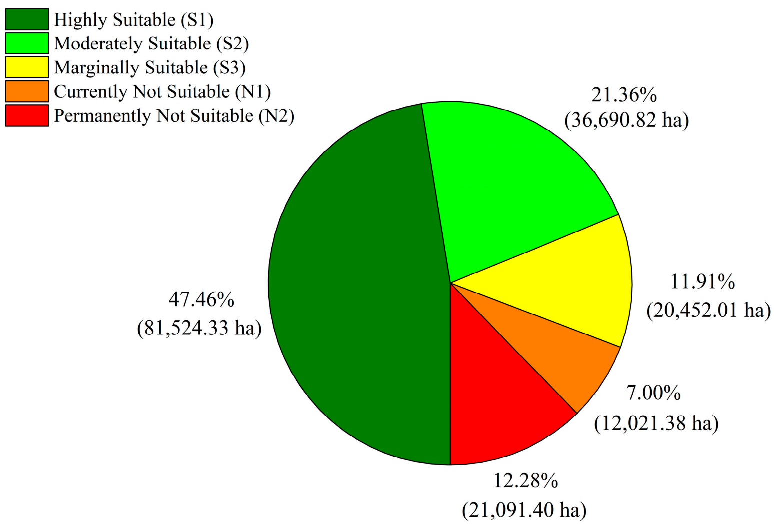

(**b**)

Figure 9. Soybean crop suitability and coverage; (**a**) map depicting the suitability of soybean cultivation; and (**b**) spatial distribution of soybean crop suitability classes across the area.

4. Discussion

4.1. Irrigation Water Suitability

In agricultural systems, water pH affects soil health and plant nutrient uptake. The high pH of the tube-well water samples collected near urban/industrial areas could be attributed to a higher propensity of soil salts to dissolve, releasing Na^+ and Ca^{2+} ions, which hinders plant growth [35]. EC (dS m^{-1}) significantly impacts soil structure and crop growth, mainly when the IW contains higher salinity [36]. The EC in tube-well water was higher than in canal water due to the accumulation of dissolved minerals in underground aquifers caused by low rainfall, high evaporation rates, and industrial effluent leaching [37]. High RSC in Chak 52 RB and 282 GB might be due to human and agricultural activities, such as overuse of Ca^{2+}- and Mg^{2+}-containing fertilizers and IW. Ahmed [38] stated that Na^+ in groundwater can be from natural sources (mineral weathering) and human activities (irrigation, industrial processes). The SAR index indicates that the available IW in the study area is safe for agriculture. Khan and Wen [39] found SAR values of 1.34 to 7.69 (mmol $L^{-1})^{1/2}$ in Faisalabad groundwater, which is below the 10 (mmol $L^{-1})^{1/2}$ safe limit suggested by Richards [12].

Irrigating crops with water from zones with high Cl^- levels can cause leaf burn, leaf scorch, and leaf tissue death, reducing crop yields. Cl^- sources include weathering silicate-rich rocks and human activities, such as industrial processes, wastewater treatment plant discharges, and road salt use [39,40]. TDS (ppm) in study area IW ranges from S2 to S3, owing to the high mineral content of canal water. According to Iqbal et al. [41], water with TDS > 1000 ppm becomes harder and more corrosive. Additionally, salt buildup in the root zone can impede water absorption and cause crop stress [42].

The study area is an agricultural hub that relies heavily on irrigation for crop production due to arid to semi-arid climatic conditions. The Lower Chenab Canal, Upper Chenab Canal, Jhang Branch Canal, Gogera Branch Canal, and groundwater irrigate the region. Marginal groundwater quality in some areas is due to improperly managed landfills, leaching of industrial effluents, excessive use of agrochemicals, and natural processes [43]. Our findings agree with those of Mukherjee et al. [44], who discovered that salinity, sodicity, magnesium hazard risks, and water toxicity are important indicators of IW suitability. Efficient water-management practices and effective strategies for irrigation must be implemented to guarantee a consistent supply of good-quality IW for the cultivation of crops in study area.

4.2. Agriculture Land Suitability

The soil analysis revealed that the study area has predominantly alkaline pH levels, which could be attributed to either soil salinity or sodicity. This increase in soil pH (>7.0) results from its location in a semi-arid region. Aimen et al. [45] noted that soils in Pakistan are typically calcareous and alkaline (pH > 7.0). Meanwhile, pH values ranging from 6.5 to 7.82, resulting in only slightly increased alkalinity levels, are considered moderately suitable for agriculture [46]. The decreasing behavior of EC_e indicates that the agricultural lands in the study area are low in soluble salts. It is possible that the mixing of soil, resulting from plowing, and irrigation of cultivated lands with canal water, contributes to the dispersion of accumulated salts in the soil. In contrast, salts in barren regions often accumulate on the surface of undisturbed soils [47].

Sodium may have substantial effects on soil properties and plant health. The SAR results revealed that soils in the S1 and S2 classes are ideal for crop production. The areas in N1 and N2, near residential and industrial sites, have high SAR values, implying that anthropogenic activities are the primary cause of elevated soil SAR, whereas S3 may be attributed to barren landscapes in addition to natural factors such as parent material and climatic conditions. Variation in soil sodicity (SAR) relates to on-site mineral weathering, natural salt accumulation, IW quality, climate, management practices, and soil OM contents [48].

The SSP (%) behavior is due to the loam-to-clay loam soil texture in the study area. According to Gharaibeh et al. [49], the SSP (%) of medium- to fine-textured soils ranges between 30 and 45%. Loam soil is a well-balanced blend of sand, silt, and clay, enabling adequate drainage, aeration, moisture retention, and nutrient supply [50]. As a result, over half of the soil in the region is designated as ideal for growing major cereal, oilseed, fodder crops, vegetables, and fruit plants.

Phosphorus is an essential nutrient for plant growth. Its availability varies spatially due to factors such as climate patterns, soil type, moisture, pH, OM, and the presence of other nutrients like Ca^{2+}, Mg^{2+}, and Zn^{2+} [51–54]. Phosphorus deficiency in the study area is caused by high soil pH, low OM (%), insufficient P-fertilizer use, arid to semi-arid climatic conditions, and soil calcareousness, which fixes phosphorus with Ca^{2+}, making it unavailable to plants. It is important to note that soil parent material, OM, chemical fertilizers, and canal water are the primary sources of K^+ in Pakistan [55]. The soils are low to moderate in plant-available K^+. These findings are consistent with those of Wakeel and Ishfaq [56], who reported that only 6% of Pakistan's cotton-growing soils had available K^+ concentrations of <80 mg kg^{-1}, while 15% had available K^+ concentrations of >120 mg kg^{-1}. Most soil samples collected from the study area contained no more than 1% OM. This is due to Pakistan's arid to semi-arid climatic conditions, vegetative cover, soil drainage, soil texture, tillage intensity, and plowing depth [57,58]. International standards consider healthy soil to have 1.2% OM, but different soil series in Pakistan have been reported to have between 0.52 to 1.38% OM [59].

The topography in and around the study area is flat (slope < 1%) with a gently sloping landscape. However, certain city areas have significantly steeper to undulating slopes due to man-made or natural structures such as embankments, buildings, or canals. The slope (%) may be slightly higher in such areas, but the overall slope is relatively low and well suited for agriculture farming. Brouwer et al. [60] stated that a slope ranging from 2% to 5% is generally deemed appropriate for agricultural purposes. The slopes in this range offer an excellent combo of drainage, erosion management, and moisture retention. The optimal slope for crop cultivation, on the other hand, can vary based on soil type, rain distribution, and the cropping pattern in the given area. According to Chen et al. [61], soil slopes over 2% often erode when subjected to farming operations.

In the study area, rapidly changing LU/LC due to urbanization and industrialization pose unusual land use planning and sustainable development challenges. Strategies to tackle these issues include sustainable farming, water management, crop selection, crop rotation, nutrient management, land reclamation and remediation, and training to increase barren land productivity [62,63]. The findings imply that the study area has huge potential for agricultural development.

Palombi and Sessa [64] found that most crops grow best between 15–30 °C (59–86 °F), with some preferring warmer or cooler temperatures. Singh et al. [65] reported that 20–27 °C is optimal for crop growth and development. This suggests that the study area has a 10-year mean annual temperature that is within the ideal range for crop growth. Crop precipitation needs vary by type and stage [66]. Generally, 500–900 mm (20–35 inches) of rain per year is suitable for many crops, but this varies with climate. The region has a semi-arid climate with 300–500 mm annual rainfall [67].

Land suitability is classified based on soil salinity, fertility, physical properties, land topography, and LU/LC. S1 land is considered non-saline, well-fertile, and physically suitable. S2 land is fertile and subsaline but can be farmed with proper techniques. S3 land has low fertility and slight salinity, requiring extra nourishment and conservation for optimal crop production. N1 land has severe soil fertility, salinity, or other physical/topographic issues that make farming difficult, whereas N2 land has additional environmental constraints that make farming impossible. Our results indicate that much of the area is suitable for farming, with varying degrees of suitability based on variables. These results have significant implications for crop cultivation and can aid in land use decisions.

These findings are consistent with the previous study conducted by SA Rashed [68] in Azad Jammu and Kashmir (AJK), who discovered that soil pH_e, EC (dS m^{-1}), OM (%), soil NPK-macro and micronutrients, and soluble ions are essential indicators of agricultural land suitability. Similarly, research by Kılıc et al. [69] emphasized the importance of elevation (m), slope (%), aspect, soil texture, and soil depth (m) in determining wheat crop suitability classes. Moreover, Kumar et al. [70] demonstrate that GIS and remote sensing techniques can identify suitable agricultural areas.

4.3. Soybean Crop Suitability

Soybean requires 400–500 mm of annual rainfall and grows at 10–36 °C temperatures, with a maximum yield at 24 °C. It prefers loam soils with pH 6.5–7.5 and can tolerate salinity of up to 5 dS m^{-1} with a 50% yield reduction. The region is suitable for climatic conditions; flat to undulating slopes and loam-to-clay loam texture are ideal for soybean growth. These results align with the findings of Vanger et al. [71], who found that climate, slope (%), LU/LC, and available nutrients are beneficial. In contrast, soil OM (%), pH, and drainage impede sustainable soybean production in the area. Radočaj et al. [72] found that machine-learning techniques accurately predicted soybean crop cultivation areas based on climate, soil health, topography, and vegetation indices. Furthermore, Salunkhe et al. [73] reported similar findings and found that weighted overlay and AHP analysis had high sensitivity in cropland suitability analysis.

These findings not only surpassed the acceptable threshold when compared against the training data but also closely aligned with similar studies. For instance, the AUC curve accuracy in the study by Fitzgibbon et al. [74] was recorded at 81%, while Ghosh [75] demonstrated validation outcomes of 73%, both of which closely resemble the outcomes of the current study. This analysis serves as a robust framework to guide agricultural decisions, aiding farmers and policymakers in identifying regions with the highest potential for successful soybean crops. By optimizing agricultural productivity and resource allocation in this way, the model can help to improve food security and sustainable agricultural practices.

4.4. Multi-Criteria Decision Making (MCDM)

The weighted overlay is a specific type of data fusion technique that plays a pivotal role in modern GIS and remote sensing research by combining different thematic layers (such as land use, slope, soil type, etc.) through weighted mathematical operations to generate a composite raster layer indicating site suitability for agriculture and urban planning [76,77]. The integration of diverse data sources, such as satellite imagery and ground-based measurements, allows for a more comprehensive and accurate understanding of the Earth's surface. This integrated approach facilitates the extraction of valuable information, supports more robust analyses, and enhances the effectiveness of decision-making processes in various fields, including agriculture, environmental monitoring, and disaster management. Recent studies by [9,78–81] have emphasized the significance of weighted overlay in improving the accuracy and scope of land suitability assessments, highlighting its indispensable role in advancing GIS and remote sensing applications for agricultural and environmental studies.

This study employed an AHP-based weighted overlay approach that effectively integrated various criteria to create a reliable model for determining soybean cropland suitability. This model exhibited a more than acceptable level of predictive accuracy. The incorporation of multiple criteria ensured a robust assessment of cropland suitability that lines with the findings of [74,75]. However, the model's sensitivity to variations in criteria and their weights emphasizes the need for refining its accuracy in future studies. Despite limitations in input data resolution and temporal dynamics, the combination of WOA and AHP offers a promising approach for guiding land-use planning and agricultural management. Continued research is essential to enhance the model's accuracy and applicability across diverse landscapes.

5. Conclusions

The findings revealed that the usefulness of IW for agriculture varied greatly depending on its source and composition. Except for unusual circumstances, canal water has lower salt levels unless it becomes contaminated by industrial and domestic waste, leading to soil salinization. Soil analysis showed that loam and clay loam are dominant soil textures in the study area, facilitating drainage, aeration, moisture retention, and nutrient supply. The results also suggested that suitability-promoting factors (soil pH, EC (dS m^{-1}), OM (%), available phosphorus, SSP (%), slope (%), and texture) and suitability-limiting factors (extractable K^+, SAR, and LU/LC) were the main factors affecting agricultural farming in the study area. In some areas, a sizable amount of the land is fallow and ideal for farming, whereas just a small portion is submerged in water and, therefore, unsuitable for agriculture. Furthermore, although barren areas only show marginal suitability for such uses, urbanized areas are permanently unfit for agricultural activity. This presents a unique set of challenges for land use planning and sustainable development. Researchers proposed strategies like sustainable farming, optimal water resource utilization, and land reclamation to tackle these issues to boost barren land productivity. The suitability of the research area for soybean crops varied throughout the spectrum, ranging from highly suitable to permanently unsuitable. The findings of this study are essential for farmers and policymakers seeking to manage irrigation water quality, agricultural productivity, and soil degradation sustainably.

6. Recommendations

Strategic approaches are required to introduce novel crops in barren lands that are marginally suitable for agriculture. Weeds and debris must be removed, and the soil should be amended if necessary. Water usage efficiency and crop yield can be maximized through modern agricultural techniques, such as drip irrigation. Overall, current findings emphasize the need for an integrated and holistic approach to land use planning and management that considers numerous stakeholders' varying requirements and interests while ensuring the sustainable use of natural resources. This method is effective for mapping the results of suitability and their relative marginality.

Supplementary Materials: The following supporting information can be downloaded at: https://www.mdpi.com/article/10.3390/land12112034/s1. See refs [82–87].

Author Contributions: N.A., M.F.S., H.R.A. and F.Y.: writing—original draft preparation and investigation. N.A., M.A.M. and M.A.A.: Data collection investigation and visualization. Z.C., M.F.S., F.R., J.S.A., S.n.M., M.S. and T.M.: writing—reviewing editing, and conceptualization. N.A., M.F.S., F.Y., X.L. and H.R.A.: software, validation, visualization, and data curation. H.R.A., Z.C. and M.F.S.: supervision, project administration, and funding acquisition. All authors have read and agreed to the published version of the manuscript.

Funding: This work was financially supported by the Projects of Major Innovation in Science & Technology of Shandong Province (2020CXGC011403 and 2021CXGC010803) and the Qingdao postdoctoral research supporting project (QDBSH20230202002) awarded to Dr. Muhammad Fahad Sardar. The authors would like to extend their sincere appreciation to the research supporting project by the National Natural Science Foundation of China (32201429).

Data Availability Statement: The authors will provide the raw data supporting the conclusions of this article upon request, without undue delay.

Acknowledgments: The authors acknowledge the Researchers Supporting Project number (RSPD20231078), King Saud University, Riyadh, Saudi Arabia.

Conflicts of Interest: The authors declare that they do not have any commercial or financial relationships that could be perceived as conflicts of interest.

References

1. Asif, S.; Ahmad, M.; Zafar, M.; Ali, N. Prospects and Potential of Fatty Acid Methyl Esters of Some Non-Edible Seed Oils for Use as Biodiesel in Pakistan. *Renew. Sustain. Energy Rev.* **2017**, *74*, 687–702.
2. Cheng, V.; Shoveller, A.K.; Huber, L.-A.; Kiarie, E.G. Comparative Protein Quality in Black Soldier Fly Larvae Meal vs. Soybean Meal and Fish Meal Using Classical Protein Efficiency Ratio (PER) Chick Growth Assay Model. *Poult. Sci.* **2023**, *102*, 102255. [CrossRef] [PubMed]

3. Abbas, G.; Imran, M.S.; Ali, M.; Jabbar, M.A.; Mustafa, A.; Sultan, Z.; Hussain, I.; Shafique, A.; Laghari, M.I.; Niazi, Z.K.; et al. Effect of Soybean Unavailability Situattions and COVID-19 on the Poultry Industry of Pakistan: A Comprehensive Analysis Problems Faced and Its Solution for Sustainable Animal Production. *Pak. J. Sci.* **2023**, *75*, 264–272. [CrossRef]
4. Pakistan Soybean Market Overview. 2023. Available online: https://www.tridge.com/intelligences/soybean/PK (accessed on 21 August 2023).
5. Digra, M.; Dhir, R.; Sharma, N. Land Use Land Cover Classification of Remote Sensing Images Based on the Deep Learning Approaches: A Statistical Analysis and Review. *Arab. J. Geosci.* **2022**, *15*, 1003. [CrossRef]
6. Özkan, B.; Dengiz, O.; Turan, İ.D. Site Suitability Analysis for Potential Agricultural Land with Spatial Fuzzy Multi-Criteria Decision Analysis in Regional Scale under Semi-Arid Terrestrial Ecosystem. *Sci. Rep.* **2020**, *10*, 22074. [CrossRef] [PubMed]
7. Mohammed, S.; Alsafadi, K.; Ali, H.; Mousavi, S.M.N.; Kiwan, S.; Hennawi, S.; Harsanyie, E.; Pham, Q.B.; Linh, N.T.T.; Ali, R. Assessment of Land Suitability Potentials for Winter Wheat Cultivation by Using a Multi Criteria Decision Support-Geographic Information System (MCDS-GIS) Approach in Al-Yarmouk Basin (Syria). *Geocarto Int.* **2022**, *37*, 1645–1663. [CrossRef]
8. Saaty, T.L. *The Analytic Hierarchy Process: Planning, Priority Setting, Resource Allocation*; McGraw-Hill International Book Company: New York, NY, USA, 1980; ISBN 978-0-07-054371-3.
9. Abdekareem, M.; Al-Arifi, N.; Abdalla, F.; Mansour, A.; El-Baz, F. Fusion of Remote Sensing Data Using GIS-Based AHP-Weighted Overlay Techniques for Groundwater Sustainability in Arid Regions. *Sustainability* **2022**, *14*, 7871. [CrossRef]
10. Radočaj, D.; Jurišić, M.; Gašparović, M.; Plaščak, I. Optimal Soybean (*Glycine max* L.) Land Suitability Using GIS-Based Multicriteria Analysis and Sentinel-2 Multitemporal Images. *Remote Sens.* **2020**, *12*, 1463. [CrossRef]
11. Kamkar, B.; Dorri, M.A.; Teixeira da Silva, J.A. Assessment of Land Suitability and the Possibility and Performance of a Canola (*Brassica napus* L.)–Soybean (*Glycine max* L.) Rotation in Four Basins of Golestan Province, Iran. *Egypt. J. Remote Sens. Space Sci.* **2014**, *17*, 95–104. [CrossRef]
12. Richards, L.A. *Diagnosis and Improvement of Saline and Alkali Soils*; US Government Printing Office: Washington, DC, USA, 1954.
13. Bouyoucos, G.J. Hydrometer Method Improved for Making Particle Size Analyses of Soils 1. *Agron. J.* **1962**, *54*, 464–465. [CrossRef]
14. USDA. *Soil Mechanics Level 1, Module 3-USDA Textural Classification*; US Department of Agriculture, Soil Conservation Service: Washington, DC, USA, 1987.
15. Blake, G.R.; Hartge, K.H. Bulk Density. In *Methods of Soil Analysis*; John Wiley & Sons, Ltd.: Hoboken, NJ, USA, 1986; pp. 363–375. ISBN 978-0-89118-864-3.
16. Walkley, A.; Black, I.A. An Examination of the Degtjareff Method for Determining Soil Organic Matter, and a Proposed Modification of the Chromic Acid Titration Method. *Soil Sci.* **1934**, *37*, 29–38. [CrossRef]
17. Olsen, S.R. *Estimation of Available Phosphorus in Soils by Extraction with Sodium Bicarbonate*; US Department of Agriculture: Washington, DC, USA, 1954.
18. Schollenberger, C.J.; Simon, R.H. Determination of Exchange Capacity and Exchangeable Bases in Soil—Ammonium Acetate Method. *Soil Sci.* **1945**, *59*, 13–24. [CrossRef]
19. Yang, C.-C. Image Enhancement by Modified Contrast-Stretching Manipulation. *Opt. Laser Technol.* **2006**, *38*, 196–201. [CrossRef]
20. Kaplan, G. Sentinel-2 Pan Sharpening—Comparative Analysis. *Proceedings* **2018**, *2*, 345. [CrossRef]
21. Issiako, D.; Arouna, O.; Soufiyanou, K.; Ismaila, T.; Tente, B. Prospective Mapping of Land Cover and Land Use in The Classified Forest of The Upper Alibori Based on Satellite Imagery. *Geoplan. J. Geomat. Plan.* **2022**, *8*, 115–126. [CrossRef]
22. Ben-David, A. Comparison of Classification Accuracy Using Cohen's Weighted Kappa. *Expert Syst. Appl.* **2008**, *34*, 825–832. [CrossRef]
23. Rwanga, S.S.; Ndambuki, J.M. Accuracy Assessment of Land Use/Land Cover Classification Using Remote Sensing and GIS. *Int. J. Geosci.* **2017**, *8*, 611. [CrossRef]
24. Foody, G.M. Explaining the Unsuitability of the Kappa Coefficient in the Assessment and Comparison of the Accuracy of Thematic Maps Obtained by Image Classification. *Remote Sens. Environ.* **2020**, *239*, 111630. [CrossRef]
25. Yilmaz, A.E.; Demirhan, H. Weighted Kappa Measures for Ordinal Multi-Class Classification Performance. *Appl. Soft Comput.* **2023**, *134*, 110020. [CrossRef]
26. Saaty, T.L. Decision Making with the Analytic Hierarchy Process. *Int. J. Serv. Sci.* **2008**, *1*, 83–98. [CrossRef]
27. Malczewski, J. *GIS and Multicriteria Decision Analysis*; John Wiley & Sons: Hoboken, NJ, USA, 1999.
28. Chen, X.; Peng, L.; Wu, Z.; Pedrycz, W. Controlling the Worst Consistency Index for Hesitant Fuzzy Linguistic Preference Relations in Consensus Optimization Models. *Comput. Ind. Eng.* **2020**, *143*, 106423. [CrossRef]
29. Prasad, V.S.; Kousalya, P. Role of Consistency in Analytic Hierarchy Process–Consistency Improvement Methods. *Indian J. Sci. Technol.* **2017**, *10*, 1–5.
30. Taoufik, M.; Fekri, A. GIS-Based Multi-Criteria Analysis of Offshore Wind Farm Development in Morocco. *Energy Convers. Manag. X* **2021**, *11*, 100103. [CrossRef]
31. Khan, A.; Ali, Y.; Pamucar, D. Solar PV Power Plant Site Selection Using a GIS-Based Non-Linear Multi-Criteria Optimization Technique. *Environ. Sci. Pollut. Res.* **2023**, *30*, 57378–57397. [CrossRef]
32. Shekar, P.R.; Mathew, A. Delineation of Groundwater Potential Zones and Identification of Artificial Recharge Sites in the Kinnerasani Watershed, India, Using Remote Sensing-GIS, AHP, and Fuzzy-AHP Techniques. *AQUA Water Infrastruct. Ecosyst. Soc.* **2023**, *72*, 1474–1498. [CrossRef]

33. Saha, S.; Mondal, P. Estimation of the Effectiveness of Multi-Criteria Decision Analysis and Machine Learning Approaches for Agricultural Land Capability in Gangarampur Subdivision, Eastern India. *Artif. Intell. Geosci.* **2022**, *3*, 179–191. [CrossRef]
34. Sulaiman, W.H.; Mustafa, Y.T. Geospatial Multi-Criteria Evaluation Using AHP–GIS to Delineate Groundwater Potential Zones in Zakho Basin, Kurdistan Region, Iraq. *Earth* **2023**, *4*, 655–675. [CrossRef]
35. Eldaw, E.; Huang, T.; Mohamed, A.K.; Mahama, Y. Classification of Groundwater Suitability for Irrigation Purposes Using a Comprehensive Approach Based on the AHP and GIS Techniques in North Kurdufan Province, Sudan. *Appl. Water Sci.* **2021**, *11*, 126. [CrossRef]
36. Hailu, B.; Mehari, H. Impacts of Soil Salinity/Sodicity on Soil-Water Relations and Plant Growth in Dry Land Areas: A Review. *J. Nat. Sci. Res.* **2021**, *12*, 1–10.
37. Ali, A. Assessment of Groundwater Quality Using Geographical Information System: A Case Study of Faisalabad, Pakistan. *J. Environ. Agric. Sci.* **2021**, *23*, 30–35.
38. Ahmed, S.; Mulhim, M.; Qureshi, F.; Akhtar, N.; Lagudu, S. Reckoning Groundwater Quality and Hydrogeochemical Processes for Drinking and Irrigation Purposes under the Influence of Anthropogenic Activities, North India. *Pollutants* **2022**, *2*, 486–509. [CrossRef]
39. Khan, M.A.; Wen, J. Evaluation of Physicochemical and Heavy Metals Characteristics in Surface Water under Anthropogenic Activities Using Multivariate Statistical Methods, Garra River, Ganges Basin, India. *Environ. Eng. Res.* **2021**, *26*, 200280. [CrossRef]
40. Kaushal, S.S.; Likens, G.E.; Pace, M.L.; Reimer, J.E.; Maas, C.M.; Galella, J.G.; Utz, R.M.; Duan, S.; Kryger, J.R.; Yaculak, A.M. Freshwater Salinization Syndrome: From Emerging Global Problem to Managing Risks. *Biogeochemistry* **2021**, *154*, 255–292. [CrossRef]
41. Iqbal, J.; Su, C.; Rashid, A.; Yang, N.; Baloch, M.Y.J.; Talpur, S.A.; Ullah, Z.; Rahman, G.; Rahman, N.U.; Sajjad, M.M. Hydrogeochemical Assessment of Groundwater and Suitability Analysis for Domestic and Agricultural Utility in Southern Punjab, Pakistan. *Water* **2021**, *13*, 3589. [CrossRef]
42. Rawat, K.S.; Singh, S.K.; Gautam, S.K. Assessment of Groundwater Quality for Irrigation Use: A Peninsular Case Study. *Appl. Water Sci.* **2018**, *8*, 233. [CrossRef]
43. Ahmad, H.R.; Sabir, M.; Zia ur Rehman, M.; Aziz, T.; Maqsood, M.A.; Ayub, M.A.; Shahzad, A. Wastewater Irrigation-Sourced Plant Nutrition: Concerns and Prospects. In *Plant Micronutrients: Deficiency and Toxicity Management*; Aftab, T., Hakeem, K.R., Eds.; Springer International Publishing: Cham, Switzerland, 2020; pp. 417–434; ISBN 978-3-030-49856-6.
44. Mukherjee, I.; Singh, U.K.; Chakma, S. Evaluation of Groundwater Quality for Irrigation Water Supply Using Multi-Criteria Decision-Making Techniques and GIS in an Agroeconomic Tract of Lower Ganga Basin, India. *J. Environ. Manag.* **2022**, *309*, 114691. [CrossRef]
45. Aimen, A.; Basit, A.; Bashir, S.; Aslam, Z.; Shahid, M.F.; Amjad, S.; Mehmood, K.; Aljuaid, B.S.; El-Shehawi, A.M.; Tan Kee Zuan, A.; et al. Sustainable Phosphorous Management in Two Different Soil Series of Pakistan by Evaluating Dynamics of Phosphatic Fertilizer Source. *Saudi J. Biol. Sci.* **2022**, *29*, 255–260. [CrossRef] [PubMed]
46. Balew, A.; Nega, W.; Legese, B.; Semaw, F. Suitable Potential Land Evaluation for Surface Water Irrigation Using Remote Sensing and GIS–MCE in the Case of Rib–Gumara Watershed, Ethiopia. *J. Indian Soc. Remote Sens.* **2021**, *49*, 2273–2290. [CrossRef]
47. Tufail, M.; Akhtar, N.; Waqas, M. Measurement of Terrestrial Radiation for Assessment of Gamma Dose from Cultivated and Barren Saline Soils of Faisalabad in Pakistan. *Radiat. Meas.* **2006**, *41*, 443–451. [CrossRef]
48. Murtaza, G.; Ghafoor, A.; Owens, G.; Qadir, M.; Kahlon, U.Z. Environmental and Economic Benefits of Saline-Sodic Soil Reclamation Using Low-Quality Water and Soil Amendments in Conjunction with a Rice–Wheat Cropping System. *J. Agron. Crop Sci.* **2009**, *195*, 124–136. [CrossRef]
49. Gharaibeh, M.A.; Albalasmeh, A.A.; El Hanandeh, A. Estimation of Saturated Paste Electrical Conductivity Using Three Modelling Approaches: Traditional Dilution Extracts; Saturation Percentage and Artificial Neural Networks. *Catena* **2021**, *200*, 105141. [CrossRef]
50. Choudhary, V.; Machavaram, R. A Comprehensive Review of Sustainable Soil Organic Growing Media for Mat-Type Paddy Seedling Nurseries Under Indian Agronomical Condition. *J. Soil Sci. Plant Nutr.* **2023**, *23*, 1515–1534. [CrossRef]
51. Hou, E.; Chen, C.; Luo, Y.; Zhou, G.; Kuang, Y.; Zhang, Y.; Heenan, M.; Lu, X.; Wen, D. Effects of Climate on Soil Phosphorus Cycle and Availability in Natural Terrestrial Ecosystems. *Glob. Chang. Biol.* **2018**, *24*, 3344–3356. [CrossRef] [PubMed]
52. Penn, C.J.; Camberato, J.J. A Critical Review on Soil Chemical Processes That Control How Soil pH Affects Phosphorus Availability to Plants. *Agriculture* **2019**, *9*, 120. [CrossRef]
53. Wahba, M.; Fawkia, L.; Zaghloul, A. Management of Calcareous Soils in Arid Region. *Int. J. Environ. Pollut. Environ. Model.* **2019**, *2*, 248–258.
54. Yang, X.; Chen, X.; Yang, X. Effect of Organic Matter on Phosphorus Adsorption and Desorption in a Black Soil from Northeast China. *Soil Tillage Res.* **2019**, *187*, 85–91. [CrossRef]
55. Wakeel, A.; Ishfaq, M.; Wakeel, A.; Ishfaq, M. Use of Potash in Pakistan. *Potash Use Dyn. Agric.* **2022**, 87–97. [CrossRef]
56. Wakeel, A.; Ishfaq, M. Promoting Precise and Balanced Use of Fertilizers in Pakistan at Farm-Gate Level. *Electron. Int. Fertil. Corresp. (e-ifc)* **2016**, *47*, 20–25.
57. Baig, M.B.; Shahid, S.A.; Straquadine, G.S. Making Rainfed Agriculture Sustainable through Environmental Friendly Technologies in Pakistan: A Review. *Int. Soil Water Conserv. Res.* **2013**, *1*, 36–52. [CrossRef]

58. Hammad, H.M.; Khaliq, A.; Abbas, F.; Farhad, W.; Fahad, S.; Aslam, M.; Shah, G.M.; Nasim, W.; Mubeen, M.; Bakhat, H.F. Comparative Effects of Organic and Inorganic Fertilizers on Soil Organic Carbon and Wheat Productivity under Arid Region. *Commun. Soil Sci. Plant Anal.* **2020**, *51*, 1406–1422. [CrossRef]
59. Azam, F.; Iqbal, M.M.; Inayatullah, C.; Malik, K.A. *Technologies for Sustainable Agriculture*; Nuclear Institute for Agriculture and Biology: Faisalabad, Pakistan, 2001.
60. Brouwer, C.; Prins, K.; Kay, M.; Heibloem, M. Irrigation Water Management: Irrigation Methods. *Train. Man.* **1988**, *9*, 5–7.
61. Chen, D.; Wei, W.; Chen, L. Effects of Terracing Practices on Water Erosion Control in China: A Meta-Analysis. *Earth-Sci. Rev.* **2017**, *173*, 109–121. [CrossRef]
62. Shah, K.K.; Modi, B.; Pandey, H.P.; Subedi, A.; Aryal, G.; Pandey, M.; Shrestha, J. Diversified Crop Rotation: An Approach for Sustainable Agriculture Production. *Adv. Agric.* **2021**, *2021*, 8924087. [CrossRef]
63. Srinivasarao, C.; Rakesh, S.; Kumar, G.R.; Manasa, R.; Somashekar, G.; Lakshmi, C.S.; Kundu, S. Soil Degradation Challenges for Sustainable Agriculture in Tropical India. *Curr. Sci.* **2021**, *120*, 492. [CrossRef]
64. Palombi, L.; Sessa, R. *Climate-Smart Agriculture: Sourcebook*; Food and Agriculture Organization of the United Nations (FAO): Rome, Italy, 2013.
65. Singh, S.; Kalia, P.; Meena, R.K.; Sharma, B.B.; Parihar, B.R. Agro-Morphological and Molecular Diversity Analysis of New Cytoplasmic Male Sterile Lines in Indian Cauliflower for Their Use in Hybrid Breeding. *Sci. Hortic.* **2022**, *301*, 111107. [CrossRef]
66. Allen, R.G.; Pereira, L.S.; Raes, D.; Smith, M. *Crop Evapotranspiration-Guidelines for Computing Crop Water Requirements-FAO Irrigation and Drainage Paper 56*; FAO: Rome, Italy, 1998; Volume 300, p. D05109.
67. Yasin, G.; Ur Rahman, S.; Farrakh Nawaz, M.; Qadir, I.; Zubair, M.; Gul, S.; Safdar Hussain, M.; Zain, M.; Athar Khaliq, M. Estimating Carbon Stocks and Biomass Accumulation in Three Different Agroforestry Patterns in the Semi-Arid Region of Pakistan. *Carbon Manag.* **2021**, *12*, 593–602. [CrossRef]
68. SA Rashed, H. Assessment of Soil Fertility and Suitability for Some Crops Using Gis and Remote Sensing Techniques. *Ann. Agric. Sci. Moshtohor* **2021**, *59*, 1065–1076. [CrossRef]
69. Kılıc, O.M.; Ersayın, K.; Gunal, H.; Khalofah, A.; Alsubeie, M.S. Combination of Fuzzy-AHP and GIS Techniques in Land Suitability Assessment for Wheat (*Triticum aestivum*) Cultivation. *Saudi J. Biol. Sci.* **2022**, *29*, 2634–2644. [CrossRef]
70. Kumar, A.; Pramanik, M.; Chaudhary, S.; Negi, M.S. Land Evaluation for Sustainable Development of Himalayan Agriculture Using RS-GIS in Conjunction with Analytic Hierarchy Process and Frequency Ratio. *J. Saudi Soc. Agric. Sci.* **2021**, *20*, 1–17. [CrossRef]
71. Vanger, N.M.; Usman, A.K.; Mohammed, H. Land Suitability Mapping for Optimum Soybean Production in Konshisha Local Government Area, Benue State, Nigeria. *J. Agric. Econ. Environ. Soc. Sci.* **2021**, *7*, 234–245. [CrossRef]
72. Radočaj, D.; Jurišić, M.; Gašparović, M.; Plaščak, I.; Antonić, O. Cropland Suitability Assessment Using Satellite-Based Biophysical Vegetation Properties and Machine Learning. *Agronomy* **2021**, *11*, 1620. [CrossRef]
73. Salunkhe, S.; Nandgude, S.; Tiwari, M.; Bhange, H.; Chavan, S.B. Land Suitability Planning for Sustainable Mango Production in Vulnerable Region Using Geospatial Multi-Criteria Decision Model. *Sustainability* **2023**, *15*, 2619. [CrossRef]
74. Fitzgibbon, A.; Pisut, D.; Fleisher, D. Evaluation of Maximum Entropy (Maxent) Machine Learning Model to Assess Relationships between Climate and Corn Suitability. *Land* **2022**, *11*, 1382. [CrossRef]
75. Ghosh, B. Spatial Mapping of Groundwater Potential Using Data-Driven Evidential Belief Function, Knowledge-Based Analytic Hierarchy Process and an Ensemble Approach. *Environ. Earth Sci.* **2021**, *80*, 625. [CrossRef]
76. Mugiyo, H.; Chimonyo, V.G.; Sibanda, M.; Kunz, R.; Masemola, C.R.; Modi, A.T.; Mabhaudhi, T. Evaluation of Land Suitability Methods with Reference to Neglected and Underutilised Crop Species: A Scoping Review. *Land* **2021**, *10*, 125. [CrossRef]
77. Anbarasu, S.; Brindha, K.; Elango, L. Multi-Influencing Factor Method for Delineation of Groundwater Potential Zones Using Remote Sensing and GIS Techniques in the Western Part of Perambalur District, Southern India. *Earth Sci. Inform.* **2020**, *13*, 317–332. [CrossRef]
78. El Behairy, R.A.; El Baroudy, A.A.; Ibrahim, M.M.; Mohamed, E.S.; Kucher, D.E.; Shokr, M.S. Assessment of Soil Capability and Crop Suitability Using Integrated Multivariate and GIS Approaches toward Agricultural Sustainability. *Land* **2022**, *11*, 1027. [CrossRef]
79. Alarifi, S.S.; Abdelkareem, M.; Abdalla, F.; Abdelsadek, I.S.; Gahlan, H.; Al-Saleh, A.M.; Alotaibi, M. Fusion of Multispectral Remote-Sensing Data through GIS-Based Overlay Method for Revealing Potential Areas of Hydrothermal Mineral Resources. *Minerals* **2022**, *12*, 1577. [CrossRef]
80. Anusha, B.N.; Babu, K.R.; Kumar, B.P.; Sree, P.P.; Veeraswamy, G.; Swarnapriya, C.; Rajasekhar, M. Integrated Studies for Land Suitability Analysis towards Sustainable Agricultural Development in Semi-Arid Regions of AP, India. *Geosyst. Geoenviron.* **2023**, *2*, 100131. [CrossRef]
81. Roy, S.; Singha, N.; Bose, A.; Basak, D.; Chowdhury, I.R. Multi-Influencing Factor (MIF) and RS–GIS-Based Determination of Agriculture Site Suitability for Achieving Sustainable Development of Sub-Himalayan Region, India. *Environ. Dev. Sustain.* **2023**, *25*, 7101–7133. [CrossRef]
82. He, L.; Jin, N.; Yu, Q. Impacts of Climate Change and Crop Management Practices on Soybean Phenology Changes in China. *Sci. Total Environ.* **2020**, *707*, 135638. [CrossRef]
83. Pearsons, K.A.; Omondi, E.C.; Heins, B.J.; Zinati, G.; Smith, A.; Rui, Y. Reducing Tillage Affects Long-Term Yields but Not Grain Quality of Maize, Soybeans, Oats, and Wheat Produced in Three Contrasting Farming Systems. *Sustainability* **2022**, *14*, 631. [CrossRef]

84. Rasheed, A.; Raza, A.; Jie, H.; Mahmood, A.; Ma, Y.; Zhao, L.; Xing, H.; Li, L.; Hassan, M.U.; Qari, S.H.; et al. Molecular Tools and Their Applications in Developing Salt-Tolerant Soybean (*Glycine max* L.) Cultivars. *Bioengineering* **2022**, *9*, 495. [CrossRef] [PubMed]
85. Merry, R.; Espina, M.J.; Lorenz, A.J.; Stupar, R.M. Development of a Controlled-Environment Assay to Induce Iron Deficiency Chlorosis in Soybean by Adjusting Calcium Carbonates, pH, and Nodulation. *Plant Methods* **2022**, *18*, 36. [CrossRef] [PubMed]
86. Koirala, P.; Thakuri, S.; Joshi, S.; Chauhan, R. Estimation of Soil Erosion in Nepal Using a RUSLE Modeling and Geospatial Tool. *Geosciences* **2019**, *9*, 147. [CrossRef]
87. Radočaj, D.; Jurišić, M.; Zebec, V.; Plaščak, I. Delineation of Soil Texture Suitability Zones for Soybean Cultivation: A Case Study in Continental Croatia. *Agronomy* **2020**, *10*, 823. [CrossRef]